

Learning with Memory-based Virtual Classes for Deep Metric Learning

Byungsoo Ko[‡]
NAVER/LINE Vision
kobiso62@gmail.com

Geonmo Gu[‡]
NAVER/LINE Vision
korgm403@gmail.com

Han-Gyu Kim
NAVER Clova Speech
hangyu.kim@navercorp.com

Abstract

The core of deep metric learning (DML) involves learning visual similarities in high-dimensional embedding space. One of the main challenges is to generalize from seen classes of training data to unseen classes of test data. Recent works have focused on exploiting past embeddings to increase the number of instances for the seen classes. Such methods achieve performance improvement via augmentation, while the strong focus on seen classes still remains. This can be undesirable for DML, where training and test data exhibit entirely different classes. In this work, we present a novel training strategy for DML called MemVir. Unlike previous works, MemVir memorizes both embedding features and class weights to utilize them as additional virtual classes. The exploitation of virtual classes not only utilizes augmented information for training but also alleviates a strong focus on seen classes for better generalization. Moreover, we embed the idea of curriculum learning by slowly adding virtual classes for a gradual increase in learning difficulty, which improves the learning stability as well as the final performance. MemVir can be easily applied to many existing loss functions without any modification. Extensive experimental results on famous benchmarks demonstrate the superiority of MemVir over state-of-the-art competitors. Code of MemVir will be publicly available.

1. Introduction

Deep metric learning (DML) is of great importance for learning visual similarities in a wide range of vision tasks, such as image clustering [17], unsupervised learning [4, 15, 5], and image retrieval [43, 10, 24, 12]. Learning visual similarity aims to build a well-generalized embedding space that reflects visual similarities of images using a defined distance metric. Typically, training and test data exhibit entirely different classes in DML. Thus, the main challenge is to maximize generalization performance from a training distribution to a shifted test distribution, which differs from classic classification tasks that deal with i.i.d.

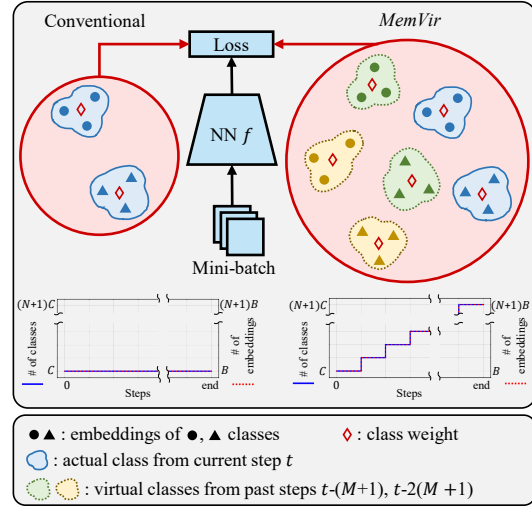


Figure 1. In conventional training, the loss function is computed with actual classes. On the other hand, in MemVir, classes from previous steps (virtual classes) are used to compute the loss function along with the actual classes. Moreover, the number of classes and embeddings are gradually increased by adding virtual classes, where C and B denote number of classes and batch size, N and M are hyper-parameters for MemVir.

training and test distributions [31, 37].

Current DML approaches focus on learning visual similarities with objective functions, which considers pairwise similarity (pair-based losses) [6, 38, 46] or similarity between samples and class representatives (proxy-based losses) [41, 40, 28, 7, 42]. Recent studies propose exploiting additional embeddings from past training steps, which are saved and controlled in the memory queue, to increase the number of samples in a mini-batch and that of hard negative pairs [15, 5, 45, 22]. And yet, these methods of utilizing past embeddings is still constrained to the seen classes of the training data. Thus, the trained model might result to over-fit to the seen classes while under-perform on the unseen classes in test data. Therefore, to learn an embedding space that generalizes, we need to alleviate the strong focus on seen classes during the training phase [37, 31, 30].

[‡] Authors contributed equally.

In this paper, we propose a novel training strategy, which trains a model with Memory-based Virtual classes (MemVir), for DML. In MemVir, we maintain memory queues for both class weights and embedding features. Instead of using them to increase the number of instances of seen classes, they are treated as virtual classes to compute the loss function along with the actual classes, as illustrated in Figure 1. Moreover, we incorporate the idea of curriculum learning (CL) to gradually increase the learning difficulty by slowly adding virtual classes. The proposed MemVir has the following advantages: **1)** MemVir trains a model with augmented information, which includes increased number of classes ($C \rightarrow (N + 1)C$) and instances ($B \rightarrow (N + 1)B$) without additional feature extraction. **2)** CL-like gradually increasing the learning difficulty improves the optimization stability and final performance. **3)** Exploiting virtual classes help achieve more generalized embedding space by alleviating excessively strong focus on seen classes of training data. **4)** MemVir can be easily applied to many existing loss functions to obtain a significant performance boost without any modification of the loss function.

Contributions. **1)** We propose a novel training strategy for DML that exploits past embeddings and class weights as virtual classes to improve generalization. We further improve the training process and performance by incorporating the idea of CL. **2)** We exhaustively analyze our proposed method and demonstrate that employing virtual classes improves generalization by alleviating a strong focus on seen classes theoretically and empirically. **3)** MemVir achieves state-of-the-art performance on three popular benchmarks of DML in both conventional and *Metric Learning Reality Check (MLRC)* [33] evaluation protocol.

2. Related Work

Sample Generation and Memory-based Learning. In DML, the generation of hard samples has been investigated to perform training with more informative samples [8, 49, 12, 24]. DAML [8] and HDML [49] utilize generative networks to generate synthetic samples, while Symm [12] and EE [24] generate synthetic samples by geometric relations. Meanwhile, utilizing information from previous steps has been explored in many computer vision tasks [15, 5, 45, 22]. In supervised DML, XBM [45] is proposed to use memorized embeddings for extending negative samples in pair-based losses. In XBM, the state difference between past and current embeddings is disregarded based on “*slow drift*” phenomena. On the other hand, [22] argues that a large accumulated error caused by the state difference may degrade the training process. They present BroadFace method for softmax variant losses to control the error by compensating the state difference and gradient control. The above-mentioned methods focus on utilizing gen-

erated or memorized information with respect to increasing the number of instances for the seen classes. However, this may result in a model overly optimized to the seen classes while under-performing on the unseen classes in test data. Rather than disregarding or controlling the state difference, the proposed MemVir exploits the state difference by employing the memorized embeddings and class weights as *virtual classes*, which are treated as different classes from the actual (seen) classes. The exploitation of virtual classes helps achieve more generalized embedding space by alleviating a strong focus on seen classes. Additional comparison with XBM w.r.t “*slow drift*” phenomena is included in supplementary Section B.2.

Virtual Class. In image recognition task, Virtual softmax [3] has been presented to enhance the discriminative property of embeddings by injecting a virtual class into the softmax loss. However, it is not only limited by a single virtual class but also cannot be used with softmax variants using l_2 -normalization. In comparison, MemVir exploits multiple virtual classes and can be used with any softmax variants and proxy-based losses.

Curriculum Learning. CL in machine learning is motivated by the idea of curriculum in human learning, where the models learn from easier samples first and more difficult samples later. Imposing CL for model training has been shown to accelerate and improve the training process in many machine learning tasks [1, 47, 13, 18]. When exploiting CL, two key factors have to be considered: (1) Scoring the difficulty of each sample; (2) scheduling the pace by which the sample is presented to the network. To define the difficulty, bootstrapping and transfer learning have been used to score the difficulty of each sample [47, 13]. For scheduling, the samples to be presented to the network can be determined in fixed or adaptive steps [47, 18]. The main difference between conventional CL and MemVir is the former schedules within the training data, whereas the latter (MemVir) increases the learning difficulty with virtual classes, which are augmented information.

3. Proposed Method

3.1. Preliminary

We define a deep neural network as $f : \mathcal{I} \rightarrow \mathcal{X}$, which is a mapping from an input data space \mathcal{I} to an embedding space \mathcal{X} . Let $X = [x_1, x_2, \dots, x_H]$ denote the D -dimensional embedding features, and each feature x_i has a corresponding label $y_i \in \{1, \dots, C\}$. The generalized form of the objective function can be written as follows:

$$\mathcal{L}(X, W) = -\frac{1}{|X|} \sum_{i=1}^{|X|} l(x_i, y_i), \quad (1)$$

where W denotes the class weights, and $l(\cdot)$ can be any of the loss functions defined below.

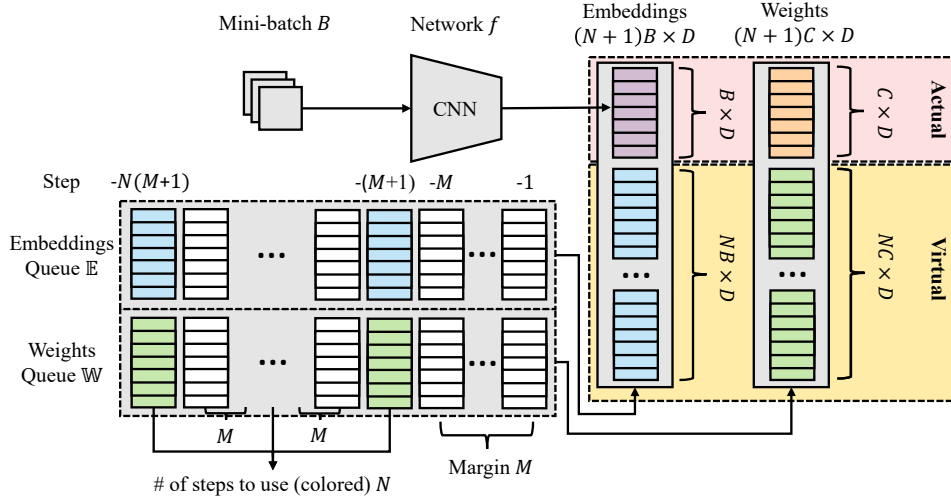


Figure 2. Overview of MemVir. Past embeddings and class weights queues are maintained. We select N steps of past embeddings and weights with margin M in between the selected steps, and use them as additional virtual classes along with actual classes for loss computation.

The most widely used classification loss function, softmax loss, has been revalued as a competitive objective function in metric learning [48, 2]. The softmax loss is used to optimize the network f and class weight W :

$$l_{softmax}(x_i, y_i) = \log \frac{e^{W_{y_i}^T x_i}}{\sum_{j=1}^C e^{W_j^T x_i}}, \quad (2)$$

where $W_j \in \mathbb{R}^D$ denotes the j -th column of weight $W \in \mathbb{R}^{D \times C}$. The bias b is set to 0 because it does not affect the performance [28, 7]. The weight W_j is the center of each class [7, 42] and serves as a representative.

For improved performance and better interpretation, [41, 40, 28] proposes to normalize weights and embedding features to lay them on a hypersphere with a fixed radius. We perform l_2 -normalization to fix the size of the weights and embedding features to the following: $\|W_j\| = 1$ and feature $\|x_i\| = 1$. Subsequently, we can simplify the logits [35] by transforming $W_j^T x_i = \|W_j\| \|x_i\| \cos \theta_j = \cos \theta_j$, and define the Norm-softmax loss as follows:

$$l_{norm}(x_i, y_i) = \log \frac{e^{\gamma \cos \theta_{y_i}}}{e^{\gamma \cos \theta_{y_i}} + \sum_{j=1, j \neq y_i}^C e^{\gamma \cos \theta_j}}, \quad (3)$$

where γ is a scale factor. The proposed method MemVir can be used with softmax variants as well as proxy-based losses because a proxy is a class representative feature much like class weights of softmax variants. Hence, we include the details of other loss functions (CosFace [42], ArcFace [7], CurricularFace [18], Proxy-NCA [32], and Proxy-Anchor [21]) in supplementary Section A.

3.2. Learning with Memory-based Virtual Classes

We propose a novel training strategy called MemVir, which trains a model with virtual classes from past steps

to exploit augmented information and obtain better generalization. When conventional metric learning trains a model with given C classes and B embeddings from training data, MemVir gradually increases the number of classes ($C \rightarrow (N+1)C$) and embeddings ($B \rightarrow (N+1)B$) with the virtual classes. We use the naming convention of MemVir(N, M), which indicates the hyper-parameters of the proposed method, to be defined below.

Queuing Past Embeddings and Weights. To form a class in loss computation, a pair of the class representative feature (weight) and embedding features are required. Hence, in MemVir, we maintain two types of memory queues: embedding queue \mathbb{E} and weight queue \mathbb{W} , where each entity of the queues is a collection of embeddings or class weights of each step as illustrated in Figure 2. For each step, the collection of embeddings X and weights W are enqueued to \mathbb{E} and \mathbb{W} , respectively. The size of each queue is determined as $N(M+1)$, where N is the number of selected steps to use for the loss computation, and M is the margin between the selected steps. The shape and position of class clusters vary by each step because the network parameters change during training process. Such variance between steps is utilized in MemVir by exploiting weights and embeddings from previous steps as virtual classes. Here, the difference between the selected steps can be controlled by the margin M .

Scheduling Usage of Virtual Classes. In MemVir, virtual classes will be utilized to gradually increase learning difficulty as CL. The scheduling of virtual class usage includes two periods: *warm-up* and *step-pacing*. We turn on MemVir and begin managing queues after the warm-up step U (epoch U_e), because the embeddings of the initial phase are typically scattered without forming clusters,

Algorithm 1: Pseudo-code of MemVir

```

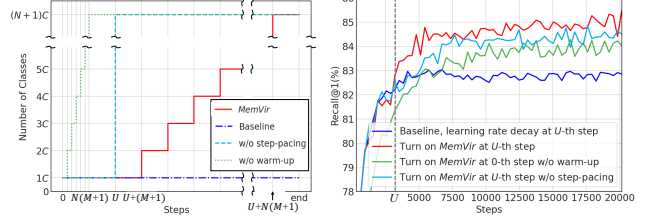
// f: encoder network
// weight/embed_queue: weight and embedding memory queue
// Ue, N, M: warm-up epoch, number of steps, margin
1 for input, label in loader do
2   embed = f.forward(input)
3   weight = f.get_class_weight()
   // Turn on MemVir when it is in use and past warm-up epoch
4   if MemVir is True and epoch ≥ Ue then
5     cur_weight = weight.copy()
6     cur_embed = embed.copy()
7     cur_label = label.copy()
   // Prepare embeddings and weights by step-pacing
   // The order of each queue is from new to old
8     if len(weight_queue) > M then
9       for idx in range(M, len(weight_queue), M + 1) do
10        pre_weight = weight_queue[idx]
11        pre_embed, pre_label = embed_queue[idx]
        // Create new label indices for virtual classes
12        new_label = create_new_label(pre_label)
13        weight.concatenate(weight, pre_weight)
14        embed.concatenate(embed, pre_embed)
15        label.concatenate(label, new_label)
16      end
   // Update memory queues
17      enqueue(weight_queue, cur_weight)
18      enqueue(embed_queue, (cur_embed, cur_label))
19      if len(weight_queue) > N(M + 1) then
20        dequeue(weight_queue)
21        dequeue(embed_queue)
   // Compute loss and back-propagation
22   loss = compute_loss(weight, embed, label)
23   loss.backward()
24   optimizer.step()
25 end

```

which can be a distraction for training. It is noteworthy that we use MemVir without learning rate decay because decaying the learning rate changes the difference between steps; thus, the learning rate decay can be used with a modification of hyper-parameter M of MemVir. After the warm-up, the step-pacing algorithm takes place by storing embeddings and weights of each step in their respective queues and reusing them for loss computations, as described in Algorithm 1. As the queue size grows, previously stored embeddings and weights from every $M + 1$ steps are selected as virtual classes when computing the loss at each step. The number of selected steps for virtual classes would increase gradually from 0 to N determined by current queue size. This results in increasing the number of classes by a staircase function, and the function s of the number of classes can be written as:

$$s(i) = \begin{cases} C, & i < U, \\ C \times \left\{ \min(\lfloor \frac{i-U}{M+1} \rfloor, N) + 1 \right\}, & i \geq U, \end{cases} \quad (4)$$

where i denotes the current step. The scheduling function of MemVir is illustrated by the red line in Figure 3a.



(a) Different ways of scheduling. (b) Performance by scheduling.

Figure 3. Impact of scheduling. (a) Different ways of scheduling for adding virtual classes. (b) Performance of each scheduling case with MemVir(5,100) and Norm-softmax as baseline on CARS196.

Learning with Multiple Virtual Classes. When we select N steps of past embeddings and weights from the queues, it indicates that we have NC virtual classes. We denote the set of selected past embeddings and weights as \tilde{X} and \tilde{W} , respectively. Subsequently, we compute the objective function with virtual classes as follows:

$$\mathcal{L}(X \cup \tilde{X}, W \cup \tilde{W}) = -\frac{1}{|X \cup \tilde{X}|} \sum_{i=1}^{|X \cup \tilde{X}|} l(x_i, y_i), \quad (5)$$

where $l(\cdot)$ can be any type of loss function. The implementation of MemVir is simple without any modification of the loss function, and it gives a significant performance improvement in DML without any additional computational cost in the inference phase.

3.3. Discussion and Analysis

3.3.1 Analysis of Scheduling

Figure 3 shows the different ways of scheduling and the performance of each case. In Figure 3a, when the MemVir is turned on at warm-up step U , it begins adding virtual classes after each $M + 1$ step, gradually. Compared with MemVir, ‘w/o warm-up’ starts adding virtual classes from the initial steps, whereas ‘w/o step-pacing’ adds all virtual classes at once after warm-up step U . For the case of ‘w/o warm-up’, training starts with degraded performance, but finally, the performance is higher than the baseline. In fact, embeddings from virtual classes at the initial steps would be scattered without forming clusters; thus, it can be a distraction at the initial steps. Meanwhile, ‘w/o step-pacing’ exhibits a slight performance degradation immediately after warm-up step U . This is because placing NC number of virtual classes simultaneously can be too difficult for training the model. By considering both cases, MemVir is able to increase the training difficulty gradually for a more stable optimization.

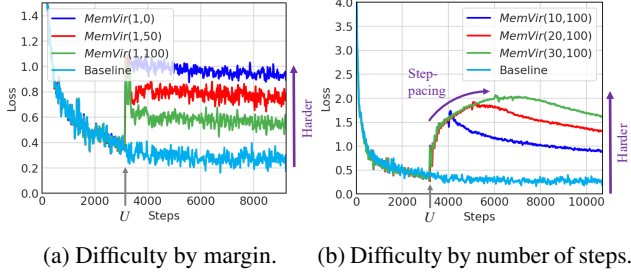


Figure 4. Impact of difficulty with Norm-softmax as baseline on CARS196. Difficulty is measured by loss value of each step. (a) Difficulty by varying margin parameter M with a fixed number of steps $N = 1$. (b) Difficulty by varying the number of steps N with a fixed margin of $M = 100$.

3.3.2 Analysis of Difficulty

MemVir controls learning difficulty via following hyper-parameters: number of steps N and margin M . To see the impact of learning difficulty by each hyper-parameter, we measure the difficulty with the loss value by following [27, 47]. As shown in Figure 4a, a smaller margin of M results in greater difficulty, which is obvious because the embeddings from the recent steps would be similar to the embeddings from the current steps. Furthermore, Figure 4b shows that adding more virtual classes increases the learning difficulty. It is noteworthy that the loss value increases slowly after warm-up step U by adding virtual classes gradually (step-pacing); subsequently, it starts decreasing after reaching a peak. The detailed performance by different hyper-parameters is presented in Section 4.4.

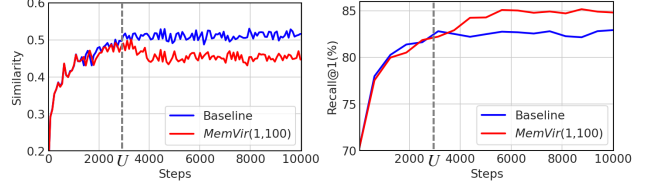
3.3.3 Gradient Analysis for Generalization

Considering the distribution shift in training and test data, strong focus on seen classes has to be alleviated in the generalization of transfer learning problems such as DML [37, 31, 30]. To demonstrate how MemVir works in generalizing models during training, we have analyzed the gradient of the softmax loss. For convenient analysis, the softmax loss in Equation 2 is re-written as follows:

$$l_{softmax}(x_i, y_i) = \log \frac{e^{\alpha(x_i, y_i)}}{\sum_{j=1}^C e^{\alpha(x_i, j)}}, \quad (6)$$

where $\alpha(x_i, j) = W_j^T x_i$. The gradient of the softmax loss over the embedding feature x_i can be inducted as follows:

$$\begin{aligned} \frac{\partial l_{softmax}(x_i, y_i)}{\partial x_i} &= W_{y_i} - \frac{\sum_{j=1}^C e^{\alpha(x_i, j)} W_j}{\sum_{j=1}^C e^{\alpha(x_i, j)}} \\ &\approx W_{y_i} - \frac{e^{\alpha(x_i, y_i)} W_{y_i}}{\sum_{j=1}^C e^{\alpha(x_i, j)}} \\ &= \tau W_{y_i}, \end{aligned} \quad (7)$$



(a) Cosine similarity (x_i, W_{y_i}) . (b) Generalization performance.

Figure 5. Generalization analysis with Norm-softmax as baseline on CARS196. (a) Similarity between embeddings and corresponding class weights of seen classes in training data. (b) Performance on unseen classes in test data.

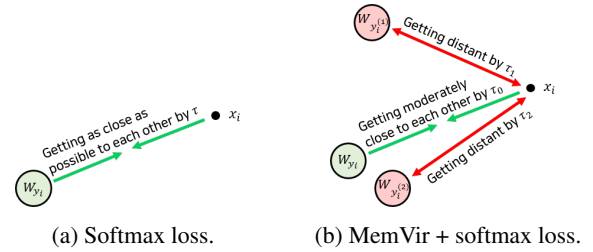


Figure 6. Illustration of an embedding (x_i) and corresponding class weight (W_{y_i}) learning, where $W_{y_i^{(n)}}$ are virtual class weights originated from the class y_i .

$$\tau = 1 - \frac{e^{\alpha(x_i, y_i)}}{\sum_{j=1}^C e^{\alpha(x_i, j)}}. \quad (8)$$

It is obvious that $\tau > 0$ and $\tau \rightarrow 0$ when $x_i \rightarrow W_{y_i}$, implying that x_i tries to get as close to W_{y_i} as possible, which is illustrated in Figure 6a. This can result in a strong focus on the target weight W_{y_i} and an over-fit to the seen classes of the training data.

In comparison, the gradient of MemVir + softmax loss over the embedding feature x_i can be inducted as follows:

$$\begin{aligned} \frac{\partial l_{MemVir}(x_i, y_i)}{\partial x_i} &= W_{y_i} - \frac{\sum_{j=1}^{(N+1)C} e^{\alpha(x_i, j)} W_j}{\sum_{j=1}^{(N+1)C} e^{\alpha(x_i, j)}} \\ &\approx W_{y_i} - \frac{\sum_{n=0}^N e^{\alpha(x_i, y_i^{(n)})} W_{y_i^{(n)}}}{\sum_{j=1}^{(N+1)C} e^{\alpha(x_i, j)}} \\ &= \tau_0 W_{y_i} + \sum_{n=1}^N \tau_n W_{y_i^{(n)}}, \end{aligned} \quad (9)$$

$$\tau_0 = 1 - \frac{e^{\alpha(x_i, y_i)}}{\sum_{j=1}^{(N+1)C} e^{\alpha(x_i, j)}}, \tau_n = - \frac{e^{\alpha(x_i, y_i^{(n)})}}{\sum_{j=1}^{(N+1)C} e^{\alpha(x_i, j)}} \quad (10)$$

where, $y_i^{(n)} (n > 0)$ are virtual classes and $y_i^{(0)} = y_i$. It is obvious that $\tau_0 > 0$. However, τ_0 would not be close to zero whether x_i is nearby W_{y_i} or not, because the denominator

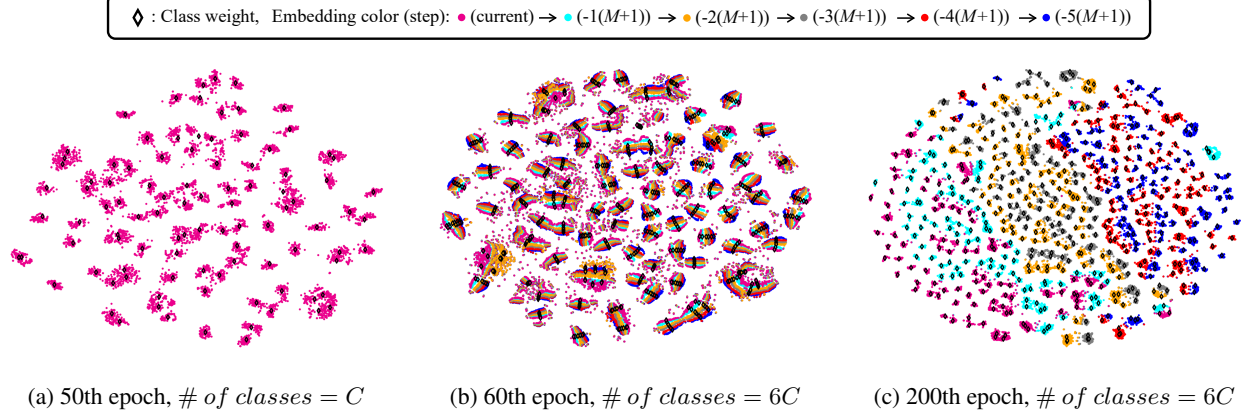


Figure 7. t-SNE visualization of 512-dimensional embedding space. Embedding features are extracted by model trained with MemVir(5,100) on CARS196 training data. Each color indicates step for embedding features.

of τ_0 would be large as the virtual classes are close to W_{y_i} . As illustrated in Figure 6b, this makes it difficult for x_i to get highly close to W_{y_i} and thus, alleviates the phenomenon of the embedding feature becoming extremely close to the target W_{y_i} . In addition, because $\tau_n < 0$, x_i tries to get farther away from the virtual classes $W_{y_i^{(n)}}$. Thus, the alleviation would be more extensive and can effectively ease the intense focus of the softmax loss, leading to a more substantial generalization. This is empirically shown in Figure 5. The baseline gradually increases the similarity between the embeddings and corresponding class weights. By contrast, when MemVir is turned on at step U , the similarity is slightly degraded by alleviating the strong focus on the seen classes, and better generalization is achieved as shown in Figure 5b. The detailed induction is provided in the supplementary Section B.1.

4. Experiments

In this section, we conduct a series of experiments to analyze and validate the effectiveness of MemVir. Please refer to the supplementary material for additional experiments: analysis of memory and computational cost (Section D.1), impact of learning rate (Section D.2), impact of warm-up (Section D.3), robustness to input deformation (Section D.4), impact of embeddings and class weights in virtual class (Section D.6), and more.

4.1. Experimental Setting

We use three popular datasets for evaluation in DML: CUB-200-2011 (CUB200) [39], CARS196 [25], and Stanford Online Products (SOP) [34]. We perform two types of evaluation procedures: *conventional evaluation* and *MLRC evaluation*. Conventional evaluation is based on the common training and evaluation procedure described in [34, 21]. All experiments are conducted on an Inception network with batch normalization [20] and a 512-dimensional

embedding feature. A batch size of 128, the Adam optimizer [23] with a learning rate of 10^{-4} , and warm-up epoch $U_e = 50$ are adopted unless otherwise noted in the experiment. Considering recent works [33, 9] that have proposed improved evaluation procedures for fairness, we include the MLRC evaluation protocol [33]. In MLRC evaluation, the procedure includes hyper-parameter search with 4-fold cross-validation, ensemble evaluation, and the usage of fair metrics (P@1, RP, and MAP@R). Please refer to supplementary Section C for details regarding the datasets and implementation.

4.2. Embedding Space Visualization

In Figure 7, we visualize the embedding space of the training data via t-SNE [29] to present how MemVir learns the embedding space. At the 50th epoch in Figure 7a, the model has been trained with only actual classes and obtains sparse embedding space with concentration on the actual classes. When all virtual classes are added at the 60th epoch in Figure 7b, virtual classes tend to be close to the actual classes and the embedding space is still sparse as in Figure 7a. This demonstrates that the model is not fully utilizing the embedding space and is highly focused on the seen classes. After enough epochs of training, at the 200th epoch in Figure 7c, the model obtains dense embedding space with sufficient discriminative power over all actual and virtual classes. To sum up, MemVir offers better utilization of embedding space by alleviating strong focus on seen classes for generalization. We include extended visualization in supplementary Section D.8.

4.3. Impact of Batch Size and Number of Classes

One advantage of MemVir is that it can utilize augmented information, including an increased number of embedding features and classes without additional feature extraction. To see the impact of the number of embedding

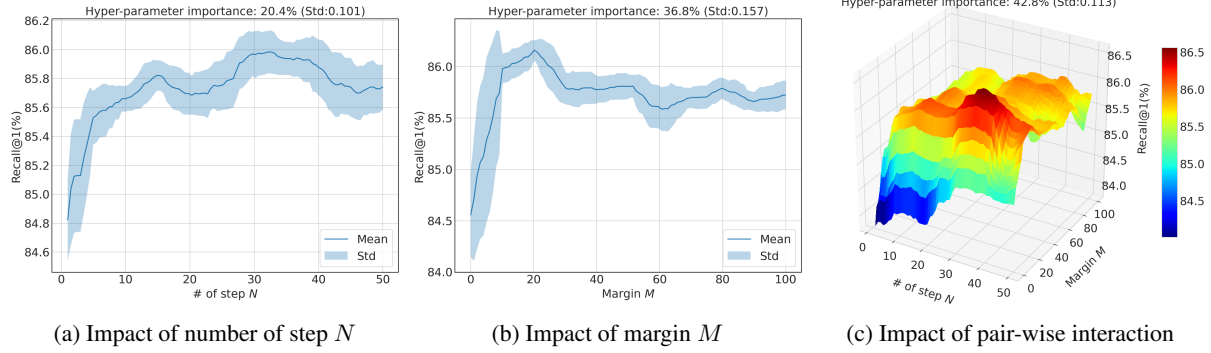


Figure 8. We use fANOVA [19] to estimate the impact of hyper-parameters. Reported performances are predicted values from random forest of fANOVA, which is trained with experimental results of MemVir on CARS196.

Batch size	8	16	32	64	128	256	512	1024
Norm-softmax	79.1	82.8	83.1	83.5	83.3	82.8	81.0	78.5
+ MemVir	80.4	<u>83.6</u>	85.0	85.5	85.0	85.0	84.8	84.6
Diff	+1.3	+0.8	+1.9	+2.0	+1.7	+2.2	+3.8	+6.1

(a) Impact of batch size.

Class ratio (%)	10	20	30	40	50	60	70	80	90	100
Norm-softmax	56.4	67.3	69.6	74.8	77.7	78.8	79.4	81.7	82.0	83.3
+ MemVir	58.5	70.1	72.8	77.2	80.0	81.3	82.6	<u>83.8</u>	84.1	85.0
Diff	+2.1	+2.8	+3.2	+2.4	+2.3	+2.5	+3.2	+2.1	+2.1	+1.7

(b) Impact of number of classes.

Table 1. Impact of batch size and number of classes on CARS196 dataset. We report Recall@1(%) performance and underline when MemVir(1,100) exceeds the best performance of the baseline Norm-softmax.

features and classes, we conduct experiments by varying the batch size and number of classes, where the training classes are randomly sampled by class ratio. As shown in Table 1a, the performance of the Norm-softmax baseline increases from the batch size of 8 to 64 and then decreases after, indicating that the increase in the batch size does not guarantee performance improvement [26, 11]. Applying MemVir to the baselines allows the models to learn with twice the number of embedding features by the virtual classes. MemVir yields performance improvement by 2.5% on average and exceeds the best performance of the baseline of batch size 64 with the batch size of only 16. Moreover, we observe that using MemVir is more robust to performance degradation due to the large batch size. As shown in Table 1b, decreasing the class ratio degrades the performance of the Norm-softmax baseline from 83.3% to 56.4%. With MemVir, which doubles the number of classes with virtual classes, we observe that the performance increases by an average of 2.4% and exceeds the best performance of the baseline with only 80% of the classes.

4.4. Impact of Hyper-parameters

For hyper-parameter analysis, we use the fANOVA framework [19], which can estimate the pattern and importance of each hyper-parameter and pair-wise interaction. We report the hyper-parameter analysis of CUB200 and SOP as well as the details of the fANOVA in the supplementary Section C.3 and D.5. As illustrated in Figure 8, the performance on CARS196 improves as the number of steps N increases. The performance improves until the margin $M = 20$, and then stabilizes after a slight degradation. However, the patterns of the impact of the hyper-parameters differ for each dataset because the characteristics of each dataset and the number of classes are diverse. We observe two common patterns among all datasets. First, a margin M larger than zero is typically better than $M = 0$; this is because classes from adjacent steps would be too similar to act as different classes and hence become distractions. Second, N exceeding one is typically better than $N = 1$. This is because by using more steps N , the effect of CL can be exploited more effectively by scheduling addition of virtual classes with a longer time.

4.5. Comparison with Related Methods

We compare MemVir with related methods from image recognition task, including the virtual class (Virtual softmax [3]), the memory-based (BroadFace [22]), and the CL (CurricularFace [18]) methods. Also, we include XBM [45] from DML to compare with BroadFace. For a fair comparison, we follow the experimental setting of [22, 18], which consists of a stochastic gradient descent (SGD) optimizer, a learning rate of 5×10^{-3} , a batch size of 512, and the ResNet50 backbone [16]. As presented in Table 3, Virtual softmax degrades the performance, whereas MemVir + softmax improves the performances of both datasets. When we combine XBM with ArcFace, we observe performance degradation when the memory size is large, as reported in BroadFace [22]. The performance can be further improved

Method	CUB200			CARS196			SOP		
	P@1	RP	MAP@R	P@1	RP	MAP@R	P@1	RP	MAP@R
Norm-softmax [41]	65.65 ± 0.30	35.99 ± 0.15	25.25 ± 0.13	83.16 ± 0.25	36.20 ± 0.26	26.00 ± 0.30	75.67 ± 0.17	50.01 ± 0.22	47.13 ± 0.22
<i>MemVir</i> + Norm-softmax	69.22 ± 0.15	37.92 ± 0.16	27.10 ± 0.13	85.81 ± 0.18	38.78 ± 0.19	28.92 ± 0.17	75.77 ± 0.20	50.24 ± 0.22	47.45 ± 0.25
CosFace [42]	67.32 ± 0.32	37.49 ± 0.21	26.70 ± 0.23	85.52 ± 0.24	37.32 ± 0.28	27.57 ± 0.30	75.79 ± 0.14	49.77 ± 0.19	46.92 ± 0.19
<i>MemVir</i> + CosFace	69.79 ± 0.26	37.85 ± 0.23	27.08 ± 0.28	87.57 ± 0.13	39.10 ± 0.21	29.56 ± 0.26	75.88 ± 0.27	49.95 ± 0.37	47.18 ± 0.38
ArcFace [7]	67.50 ± 0.25	37.31 ± 0.21	26.45 ± 0.20	85.44 ± 0.28	37.02 ± 0.29	27.22 ± 0.30	76.20 ± 0.27	50.27 ± 0.38	47.41 ± 0.40
<i>MemVir</i> + ArcFace	69.33 ± 0.41	37.82 ± 0.28	26.96 ± 0.25	88.02 ± 0.18	39.12 ± 0.15	29.63 ± 0.15	76.05 ± 0.30	50.56 ± 0.33	47.75 ± 0.32
Proxy-NCA [32]	65.69 ± 0.43	35.14 ± 0.26	24.21 ± 0.27	83.56 ± 0.27	35.62 ± 0.28	25.38 ± 0.31	75.89 ± 0.17	50.10 ± 0.22	47.22 ± 0.21
<i>MemVir</i> + Proxy-NCA	69.25 ± 0.32	37.31 ± 0.12	26.43 ± 0.17	87.02 ± 0.15	38.51 ± 0.15	28.76 ± 0.16	76.97 ± 0.31	50.81 ± 0.26	48.02 ± 0.27
Proxy-anchor [21]	69.73 ± 0.31	38.23 ± 0.37	27.44 ± 0.35	86.20 ± 0.21	39.08 ± 0.31	29.37 ± 0.29	75.37 ± 0.15	50.19 ± 0.14	47.25 ± 0.15
<i>MemVir</i> + Proxy-anchor	69.81 ± 0.28	38.57 ± 0.14	27.83 ± 0.16	86.40 ± 0.18	40.27 ± 0.20	30.58 ± 0.20	77.80 ± 0.17	53.21 ± 0.12	50.35 ± 0.13

Table 2. [MLRC evaluation] Performance (%) on three famous datasets in image retrieval task. We report the performance of concatenated 512-dim over 10 training runs. Bold numbers indicate the best score within the same loss and dataset.

Method	CARS196			SOP		
	R@1	R@2	R@4	R@1	R@10	R@100
SoftMax	78.3	86.4	91.9	76.6	89.4	95.8
Virtual SoftMax	75.1	84.1	90.1	74.5	87.9	94.8
<i>MemVir</i> + SoftMax	79.2	87.0	92.1	78.9	90.6	96.2
ArcFace	78.8	86.4	91.7	76.9	89.1	95.0
XBM + ArcFace	78.9	86.2	91.9	78.1	89.7	95.8
BroadFace + ArcFace	79.5	87.3	92.0	80.2	91.0	95.9
<i>MemVir</i> + ArcFace	80.7	88.1	92.7	80.8	91.3	96.5
CurricularFace	79.9	87.3	92.0	79.8	90.7	95.6
<i>MemVir</i> + CurricularFace	81.0	87.9	92.9	81.3	91.7	98.8

Table 3. Performance (%) comparison with related methods on CARS196 and SOP dataset.

by adding compensation technique and gradient control presented in BroadFace. However, exploiting the memorized features as virtual classes in *MemVir* shows a higher performance boost than just utilizing them for the increased number of instances in XBM and BroadFace. Considering that CurricularFace has already included the idea of CL, *MemVir* can improve the performance even further by providing virtual classes as harder cases. Moreover, it is noteworthy that the experimental results show the flexibility of *MemVir* for different types of backbones and optimizers. Extended experiments with different experimental settings are presented in the supplementary Section D.7.

4.6. Comparison with State-of-the-art

Finally, we compare the proposed method with state-of-the-art methods in DML. In the conventional evaluation shown in Table 4, every softmax variant and proxy-based loss combined with *MemVir* show significantly improved performance in every dataset. The average performance improvements are 2.3%, 3.4%, and 1.1% for CUB200, CARS196 and SOP, respectively. In comparison with the memory-based (XBM), sample generation (Symm, EE), and other recent methods (MS, SoftTriple and ProxyGML), *MemVir* shows competitive performance in all datasets. Even in the MLRC evaluation shown in Table 2, which is specifically designed in terms of fairness, *MemVir* improves performance in every dataset and metric substan-

Method	CUB200	CARS196	SOP
Multi-similarity (MS) [†] [44]	64.5	82.1	76.3
SoftTriple [36]	65.4	84.5	78.3
ProxyGML [50]	66.6	85.5	78.0
Symm [12] + MS [38]	64.9	82.4	76.9
EE [24] + MS [44]	65.1	82.9	77.0
XBM [45] + Contrastive [14]	65.8	82.0	79.5
Softmax	64.2	81.5	76.3
<i>MemVir</i> + Softmax	66.8 (+2.6)	86.5 (+5.0)	77.8 (+1.5)
Norm-softmax [41]	64.9	83.3	78.6
<i>MemVir</i> + Norm-softmax	67.3 (+2.4)	86.8 (+3.5)	79.6 (+1.0)
CosFace [42]	65.7	83.6	78.6
<i>MemVir</i> + CosFace	67.7 (+2.0)	86.6 (+3.0)	79.7 (+1.1)
ArcFace [7]	66.1	83.7	78.8
<i>MemVir</i> + ArcFace	67.4 (+1.3)	86.5 (+2.8)	80.0 (+1.2)
Proxy-NCA [32]	64.3	82.0	78.1
<i>MemVir</i> + Proxy-NCA	68.3 (+4.0)	86.5 (+4.5)	79.2 (+1.1)
Proxy-anchor [†] [21]	67.7	84.9	78.9
<i>MemVir</i> + Proxy-anchor	69.0 (+1.3)	86.7 (+1.8)	79.7 (+0.8)

Table 4. [Conventional evaluation] Recall@1 (%) on three famous datasets in image retrieval task. [†] denotes evaluation in a fair setting described in supplementary Section C.2.1.

tially. These results demonstrate the flexibility and effectiveness of *MemVir* in DML. Please refer to the supplementary Section D.9 for extended results of the metrics and comparisons with existing methods in conventional evaluation, as well as additional performance report of separated 128-dim in MLRC evaluation.

5. Conclusion

In this paper, we have presented a novel training strategy that exploits memory-based virtual classes and incorporates the idea of CL. Theoretical and empirical analysis demonstrates that employing virtual classes as augmented information help achieve better generalization by alleviating a strong focus on seen classes. Furthermore, we show that gradually increasing the learning difficulty by slowly adding virtual classes improves the training process and final performance. Considering that *MemVir* is easily applicable to existing loss functions for better generalization, it is hence a competitive training strategy in DML.

Acknowledgement. We would like to thank all members of Visual Search team at NAVER/LINE for helpful comments and feedback. We are grateful to Yoonjae Cho, Tae Kwan Lee, and Jingeun Lee for the detailed review of the paper.

References

- [1] Yoshua Bengio, Jérôme Louradour, Ronan Collobert, and Jason Weston. Curriculum learning. In *Proceedings of the 26th annual international conference on machine learning*, pages 41–48, 2009. [2](#)
- [2] Malik Boudiaf, Jérôme Rony, Imtiaz Masud Ziko, Eric Granger, Marco Pedersoli, Pablo Piantanida, and Ismail Ben Ayed. A unifying mutual information view of metric learning: cross-entropy vs. pairwise losses. *arXiv preprint arXiv:2003.08983*, 2020. [3](#)
- [3] Binghui Chen, Weihong Deng, and Haifeng Shen. Virtual class enhanced discriminative embedding learning. In *Advances in Neural Information Processing Systems*, pages 1942–1952, 2018. [2, 7](#)
- [4] Ting Chen, Simon Kornblith, Mohammad Norouzi, and Geoffrey Hinton. A simple framework for contrastive learning of visual representations. *arXiv preprint arXiv:2002.05709*, 2020. [1](#)
- [5] Xinlei Chen, Haoqi Fan, Ross Girshick, and Kaiming He. Improved baselines with momentum contrastive learning. *arXiv preprint arXiv:2003.04297*, 2020. [1, 2](#)
- [6] Sumit Chopra, Raia Hadsell, and Yann LeCun. Learning a similarity metric discriminatively, with application to face verification. In *2005 IEEE Computer Society Conference on Computer Vision and Pattern Recognition (CVPR'05)*, volume 1, pages 539–546. IEEE, 2005. [1](#)
- [7] Jiankang Deng, Jia Guo, Niannan Xue, and Stefanos Zafeiriou. Arcface: Additive angular margin loss for deep face recognition. In *Proceedings of the IEEE Conference on Computer Vision and Pattern Recognition*, pages 4690–4699, 2019. [1, 3, 8](#)
- [8] Yueqi Duan, Wenzhao Zheng, Xudong Lin, Jiwen Lu, and Jie Zhou. Deep adversarial metric learning. In *Proceedings of the IEEE Conference on Computer Vision and Pattern Recognition*, pages 2780–2789, 2018. [2](#)
- [9] Istvan Fehervari, Avinash Ravichandran, and Srikanth Apalaraju. Unbiased evaluation of deep metric learning algorithms. *arXiv preprint arXiv:1911.12528*, 2019. [6](#)
- [10] Albert Gordo, Jon Almazán, Jerome Revaud, and Diane Larlus. Deep image retrieval: Learning global representations for image search. In *European conference on computer vision*, pages 241–257. Springer, 2016. [1](#)
- [11] Priya Goyal, Piotr Dollár, Ross Girshick, Pieter Noordhuis, Lukasz Wesolowski, Aapo Kyrola, Andrew Tulloch, Yangqing Jia, and Kaiming He. Accurate, large mini-batch sgd: Training imagenet in 1 hour. *arXiv preprint arXiv:1706.02677*, 2017. [7](#)
- [12] Geonmo Gu and Byungsoo Ko. Symmetrical synthesis for deep metric learning. *arXiv preprint arXiv:2001.11658*, 2020. [1, 2, 8](#)
- [13] Guy Hacohen and Daphna Weinshall. On the power of curriculum learning in training deep networks. *arXiv preprint arXiv:1904.03626*, 2019. [2](#)
- [14] Raia Hadsell, Sumit Chopra, and Yann LeCun. Dimensionality reduction by learning an invariant mapping. In *2006 IEEE Computer Society Conference on Computer Vision and Pattern Recognition (CVPR'06)*, volume 2, pages 1735–1742. IEEE, 2006. [8](#)
- [15] Kaiming He, Haoqi Fan, Yuxin Wu, Saining Xie, and Ross Girshick. Momentum contrast for unsupervised visual representation learning. In *Proceedings of the IEEE/CVF Conference on Computer Vision and Pattern Recognition*, pages 9729–9738, 2020. [1, 2](#)
- [16] Kaiming He, Xiangyu Zhang, Shaoqing Ren, and Jian Sun. Deep residual learning for image recognition. In *Proceedings of the IEEE conference on computer vision and pattern recognition*, pages 770–778, 2016. [7](#)
- [17] John R Hershey, Zhuo Chen, Jonathan Le Roux, and Shinji Watanabe. Deep clustering: Discriminative embeddings for segmentation and separation. In *2016 IEEE International Conference on Acoustics, Speech and Signal Processing (ICASSP)*, pages 31–35. IEEE, 2016. [1](#)
- [18] Yuge Huang, Yuhang Wang, Ying Tai, Xiaoming Liu, Pengcheng Shen, Shaoxin Li, Jilin Li, and Feiyue Huang. Curricularface: adaptive curriculum learning loss for deep face recognition. In *Proceedings of the IEEE/CVF Conference on Computer Vision and Pattern Recognition*, pages 5901–5910, 2020. [2, 3, 7](#)
- [19] Frank Hutter, Holger Hoos, and Kevin Leyton-Brown. An efficient approach for assessing hyperparameter importance. In *International conference on machine learning*, pages 754–762. PMLR, 2014. [7](#)
- [20] Sergey Ioffe and Christian Szegedy. Batch normalization: Accelerating deep network training by reducing internal covariate shift. *arXiv preprint arXiv:1502.03167*, 2015. [6](#)
- [21] Sungyeon Kim, Dongwon Kim, Minsu Cho, and Suha Kwak. Proxy anchor loss for deep metric learning. *arXiv preprint arXiv:2003.13911*, 2020. [3, 6, 8](#)
- [22] Yonghyun Kim, Wonpyo Park, and Jongju Shin. Broadface: Looking at tens of thousands of people at once for face recognition. *arXiv preprint arXiv:2008.06674*, 2020. [1, 2, 7](#)
- [23] Diederik P Kingma and Jimmy Ba. Adam: A method for stochastic optimization. *arXiv preprint arXiv:1412.6980*, 2014. [6](#)
- [24] Byungsoo Ko and Geonmo Gu. Embedding expansion: Augmentation in embedding space for deep metric learning. In *Proceedings of the IEEE/CVF Conference on Computer Vision and Pattern Recognition*, pages 7255–7264, 2020. [1, 2, 8](#)
- [25] Jonathan Krause, Michael Stark, Jia Deng, and Li Fei-Fei. 3d object representations for fine-grained categorization. In *Proceedings of the IEEE international conference on computer vision workshops*, pages 554–561, 2013. [6](#)
- [26] Alex Krizhevsky. One weird trick for parallelizing convolutional neural networks. *arXiv preprint arXiv:1404.5997*, 2014. [7](#)
- [27] M Pawan Kumar, Benjamin Packer, and Daphne Koller. Self-paced learning for latent variable models. In *Advances in*

- neural information processing systems, pages 1189–1197, 2010. 5
- [28] Weiyang Liu, Yandong Wen, Zhiding Yu, Ming Li, Bhiksha Raj, and Le Song. Sphereface: Deep hypersphere embedding for face recognition. In *Proceedings of the IEEE conference on computer vision and pattern recognition*, pages 212–220, 2017. 1, 3
- [29] Laurens van der Maaten and Geoffrey Hinton. Visualizing data using t-sne. *Journal of machine learning research*, 9(Nov):2579–2605, 2008. 6
- [30] Timo Milbich, Karsten Roth, Homanga Bharadhwaj, Samarth Sinha, Yoshua Bengio, Björn Ommer, and Joseph Paul Cohen. Diva: Diverse visual feature aggregation for deep metric learning. *arXiv preprint arXiv:2004.13458*, 2020. 1, 5
- [31] Timo Milbich, Karsten Roth, Biagio Brattoli, and Björn Ommer. Sharing matters for generalization in deep metric learning. *arXiv preprint arXiv:2004.05582*, 2020. 1, 5
- [32] Yair Movshovitz-Attias, Alexander Toshev, Thomas K Leung, Sergey Ioffe, and Saurabh Singh. No fuss distance metric learning using proxies. In *Proceedings of the IEEE International Conference on Computer Vision*, pages 360–368, 2017. 3, 8
- [33] Kevin Musgrave, Serge Belongie, and Ser-Nam Lim. A metric learning reality check. *arXiv preprint arXiv:2003.08505*, 2020. 2, 6
- [34] Hyun Oh Song, Yu Xiang, Stefanie Jegelka, and Silvio Savarese. Deep metric learning via lifted structured feature embedding. In *Proceedings of the IEEE conference on computer vision and pattern recognition*, pages 4004–4012, 2016. 6
- [35] Gabriel Pereyra, George Tucker, Jan Chorowski, Łukasz Kaiser, and Geoffrey Hinton. Regularizing neural networks by penalizing confident output distributions. *arXiv preprint arXiv:1701.06548*, 2017. 3
- [36] Qi Qian, Lei Shang, Baigui Sun, Juhua Hu, Hao Li, and Rong Jin. Softtriple loss: Deep metric learning without triplet sampling. In *Proceedings of the IEEE International Conference on Computer Vision*, pages 6450–6458, 2019. 8
- [37] Karsten Roth, Timo Milbich, Samarth Sinha, Prateek Gupta, Bjoern Ommer, and Joseph Paul Cohen. Revisiting training strategies and generalization performance in deep metric learning. *arXiv preprint arXiv:2002.08473*, 2020. 1, 5
- [38] Kihyuk Sohn. Improved deep metric learning with multi-class n-pair loss objective. In *Advances in neural information processing systems*, pages 1857–1865, 2016. 1, 8
- [39] Catherine Wah, Steve Branson, Peter Welinder, Pietro Perona, and Serge Belongie. The caltech-ucsd birds-200-2011 dataset. 2011. 6
- [40] Feng Wang, Jian Cheng, Weiyang Liu, and Haijun Liu. Additive margin softmax for face verification. *IEEE Signal Processing Letters*, 25(7):926–930, 2018. 1, 3
- [41] Feng Wang, Xiang Xiang, Jian Cheng, and Alan Loddon Yuille. Normface: L2 hypersphere embedding for face verification. In *Proceedings of the 25th ACM international conference on Multimedia*, pages 1041–1049, 2017. 1, 3, 8
- [42] Hao Wang, Yitong Wang, Zheng Zhou, Xing Ji, Dihong Gong, Jingchao Zhou, Zhifeng Li, and Wei Liu. Cosface: Large margin cosine loss for deep face recognition. In *Proceedings of the IEEE Conference on Computer Vision and Pattern Recognition*, pages 5265–5274, 2018. 1, 3, 8
- [43] Jiang Wang, Yang Song, Thomas Leung, Chuck Rosenberg, Jingbin Wang, James Philbin, Bo Chen, and Ying Wu. Learning fine-grained image similarity with deep ranking. In *Proceedings of the IEEE Conference on Computer Vision and Pattern Recognition*, pages 1386–1393, 2014. 1
- [44] Xun Wang, Xintong Han, Weilin Huang, Dengke Dong, and Matthew R Scott. Multi-similarity loss with general pair weighting for deep metric learning. In *Proceedings of the IEEE Conference on Computer Vision and Pattern Recognition*, pages 5022–5030, 2019. 8
- [45] Xun Wang, Haozhi Zhang, Weilin Huang, and Matthew R Scott. Cross-batch memory for embedding learning. In *Proceedings of the IEEE/CVF Conference on Computer Vision and Pattern Recognition*, pages 6388–6397, 2020. 1, 2, 7, 8
- [46] Kilian Q Weinberger and Lawrence K Saul. Distance metric learning for large margin nearest neighbor classification. *Journal of Machine Learning Research*, 10(Feb):207–244, 2009. 1
- [47] Daphna Weinshall, Gad Cohen, and Dan Amir. Curriculum learning by transfer learning: Theory and experiments with deep networks. *arXiv preprint arXiv:1802.03796*, 2018. 2, 5
- [48] Andrew Zhai and Hao-Yu Wu. Classification is a strong baseline for deep metric learning. *arXiv preprint arXiv:1811.12649*, 2018. 3
- [49] Wenzhao Zheng, Zhaodong Chen, Jiwen Lu, and Jie Zhou. Hardness-aware deep metric learning. In *Proceedings of the IEEE Conference on Computer Vision and Pattern Recognition*, pages 72–81, 2019. 2
- [50] Yuehua Zhu, Muli Yang, Cheng Deng, and Wei Liu. Fewer is more: A deep graph metric learning perspective using fewer proxies. *arXiv preprint arXiv:2010.13636*, 2020. 8

Learning with Memory-based Virtual Classes for Deep Metric Learning

Supplementary Material

Contents

A Loss Functions	ii
B Details of MemVir	iii
B.1. Proof of Gradient Analysis for Generalization	iii
B.2. Revisiting Slow Drift Phenomena	iv
C Details of Experimental Settings	vi
C.1. Datasets	vi
C.2. Implementation	vi
C.2.1 Conventional Evaluation	vi
C.2.2 MLRC Evaluation	vii
C.3. fANOVA	vii
D Extended Experiments	vii
D.1. Analysis of Memory and Computational Cost	vii
D.2. Impact of Learning Rate	vii
D.3. Impact of Warm-up	viii
D.4. Robustness to Input Deformation	viii
D.5. Impact of Hyper-parameters	ix
D.6. Impact of Embeddings and Class Weights in Virtual Class	ix
D.7. Comparison with Related Methods	ix
D.8. Visualization of Embedding Space	x
D.9. Comparison with State-of-the-art	xi
References	xv

A. Loss Functions

In this section, we briefly describe softmax variant and proxy-based losses used in our study, as well as the hyper-parameters of each loss. For notation, we refer to the embedding features as x_i and corresponding label as y_i . Each loss function $l(\cdot)$ is written based on the generalized form of objective function:

$$\mathcal{L}(X, W) = -\frac{1}{|X|} \sum_{i=1}^{|X|} l(x_i, y_i), \quad (\text{i})$$

where X and W are sets of embedding features and class weights, respectively.

Proxy-NCA [19] Typically, pair-based losses suffer from sampling issues such that sampling tuples heavily affects the training convergence. To address this problem, Proxy-NCA loss introduces class proxies, which represent each class. In this way, we can sample only one anchor and compare it against the corresponding positive and negative class proxies. It is noteworthy that class proxies have the same meaning as class weights from the softmax variants theoretically and practically; thus, we use the term ‘class weights’ to include class representatives or proxies in this paper. The Proxy-NCA loss can be formulated as:

$$l_{\text{proxy-NCA}}(x_i, y_i) = \log \frac{e^{-d(x_i, W_{y_i})}}{\sum_{j=1}^C e^{-d(x_i, W_j)}}, \quad (\text{ii})$$

where $d(a, b) = \|a - b\|_2$ is the Euclidean distance between a and b .

Proxy-anchor [11] Unlike typical softmax variants and proxy-based losses, Proxy-anchor loss uses each proxy as an anchor and considers its relations with all samples in a batch. We define X_w^+ and X_w^- as the set of positive and negative embedding features of each proxy (class weight) w , respectively, and W^+ as the set of positive proxies of data in the mini-batch. Because of its peculiar structure, we formulate the Proxy-anchor loss based on the mini-batch as follows:

$$\mathcal{L}_{\text{proxy-anchor}}(X, W) = \frac{1}{|W^+|} \sum_{w \in W^+} \log \left\{ 1 + \sum_{x \in X_w^+} e^{-\gamma(s(x, w) - \delta)} \right\} + \frac{1}{|W|} \sum_{w \in W} \log \left\{ 1 + \sum_{x \in X_w^-} e^{\gamma(s(x, w) + \delta)} \right\}, \quad (\text{iii})$$

where $s(a, b) = a^T b$ denotes the cosine similarity between a and b , γ is a scaling factor, and δ is a margin parameter. We use $\gamma = 46$ and $m = 0.1$ for our hyper-parameters.

CosFace [29] CosFace loss reformulates the softmax loss as a cosine loss by l_2 normalizing the embedding features and class weights, which is equivalent to the Norm-softmax loss, and defines a decision margin in cosine space as:

$$l_{\text{cosface}}(x_i, y_i) = \log \frac{e^{\gamma(\cos(\theta_{y_i}) - m)}}{e^{\gamma(\cos(\theta_{y_i}) - m)} + \sum_{j=1, j \neq y_i}^C e^{\gamma \cos \theta_j}}, \quad (\text{iv})$$

where γ is a scale and m is a margin parameter. For our hyper-parameters, we use $\gamma = 28$ and $m = 0.1$.

ArcFace [2] Similar to CosFace loss, ArcFace loss transforms the Norm-softmax loss function by applying an angular margin between the embedding x_i and the corresponding class weight W_{y_i} for each class. ArcFace loss can be formulated as:

$$l_{\text{arcface}}(x_i, y_i) = \log \frac{e^{\gamma \cos(\theta_{y_i} + m)}}{e^{\gamma \cos(\theta_{y_i} + m)} + \sum_{j=1, j \neq y_i}^C e^{\gamma \cos \theta_j}}, \quad (\text{v})$$

where we use the scale $\gamma = 24$ and the margin $m = 0.1$.

CurricularFace [7] CurricularFace incorporates the idea of curriculum learning into the ArcFace loss to adjust the relative importance of easy and hard samples during training. The loss function of CurricularFace is formulated as follows:

$$l_{curricularface}(x_i, y_i) = \log \frac{e^{\gamma T(\cos \theta_{y_i})}}{e^{\gamma T(\cos \theta_{y_i})} + \sum_{j=1, j \neq y_i}^C e^{\gamma N(t, \cos \theta_j)}}, \quad (\text{vi})$$

$$T(\cos \theta_{y_i}) = \cos(\theta_{y_i} + m), \quad (\text{vii})$$

$$N(t, \cos \theta_{y_j}) = \begin{cases} \cos \theta_{y_j}, & T(\cos \theta_{y_i}) - \cos \theta_j \geq 0 \\ \cos \theta_{y_j}(t^{(k)} + \cos \theta_j), & T(\cos \theta_{y_i}) - \cos \theta_j < 0, \end{cases} \quad (\text{viii})$$

where $T(\cdot)$ and $N(\cdot)$ are modulation functions for the positive and negative cosine similarities, respectively. The parameter $t^{(k)}$ of the k -th step is computed as follows:

$$t^{(k)} = \alpha r^{(k)} + (1 - \alpha)t^{(k)}, \quad (\text{ix})$$

where $r^{(k)}$ is the average of the positive cosine similarities and α is the momentum parameter. For our hyper-parameters, we use $\alpha = 0.99$, $\gamma = 26$ and $m = 0.3$.

B. Details of MemVir

B.1. Proof of Gradient Analysis for Generalization

We provide a detailed proof of gradient analysis for generalization, which is discussed in Section 3.3.3. The proof is shown by comparing the gradient descent of softmax and MemVir.

Gradient Descent of Softmax: As mentioned in Equation 6 of the main paper, the softmax loss can be written as follows:

$$l_{softmax}(x_i, y_i) = \log \frac{e^{\alpha(x_i, y_i)}}{\sum_{j=1}^C e^{\alpha(x_i, j)}}, \quad (\text{x})$$

where $\alpha(x_i, j) = W_j^T x_i$. The gradient of the softmax loss over the embedding feature x_i can be inducted as follows:

$$\begin{aligned} \frac{\partial l_{softmax}(x_i, y_i)}{\partial x_i} &= \frac{\sum_{j=1}^C e^{\alpha(x_i, j)} W_{y_i} e^{\alpha(x_i, y_i)} \sum_{j=1}^C e^{\alpha(x_i, j)} - e^{\alpha(x_i, y_i)} \sum_{j=1}^C W_j e^{\alpha(x_i, j)}}{e^{\alpha(x_i, y_i)} (\sum_{j=1}^C e^{\alpha(x_i, j)})^2} \\ &= W_{y_i} - \frac{\sum_{j=1}^C e^{\alpha(x_i, j)} W_j}{\sum_{j=1}^C e^{\alpha(x_i, j)}}. \end{aligned} \quad (\text{xi})$$

During training process, $e^{\alpha(x_i, y_i)} \gg e^{\alpha(x_i, j)}$ for $j \neq y_i$. By applying such conclusion to the numerator of Equation xi for approximation, following equation can be achieved:

$$\begin{aligned} \frac{\partial l_{softmax}(x_i, y_i)}{\partial x_i} &= W_{y_i} - \frac{\sum_{j=1}^C e^{\alpha(x_i, j)} W_j}{\sum_{j=1}^C e^{\alpha(x_i, j)}} \\ &\approx W_{y_i} - \frac{e^{\alpha(x_i, y_i)} W_{y_i}}{\sum_{j=1}^C e^{\alpha(x_i, j)}} \\ &= \tau W_{y_i}, \end{aligned} \quad (\text{xii})$$

$$\tau = 1 - \frac{e^{\alpha(x_i, y_i)}}{\sum_{j=1}^C e^{\alpha(x_i, j)}}. \quad (\text{xiii})$$

It is obvious that $\tau > 0$ and $\tau \rightarrow 0$ when $x_i \rightarrow W_{y_i}$, implying that x_i converges as close to W_{y_i} as possible. This can result in a strong focus on the target weight W_{y_i} and an over-fit to the seen classes of the training data.

Gradient Descent of MemVir: For MemVir, the softmax function in Equation x should be re-written as follows:

$$l_{softmax}(x_i, y_i) = \log \frac{e^{\alpha(x_i, y_i)}}{\sum_{j=1}^{(N+1)C} e^{\alpha(x_i, j)}}, \quad (\text{xiv})$$

where the number of class weights increase from C to $(N+1)C$ compared to softmax because of the existence of the virtual classes. Then, the gradient of MemVir + softmax loss over the embedding feature x_i can be inducted as follows:

$$\begin{aligned} \frac{\partial l_{MemVir}(x_i, y_i)}{\partial x_i} &= \frac{\sum_{j=1}^{(N+1)C} e^{\alpha(x_i, j)} W_{y_i} e^{\alpha(x_i, y_i)} \sum_{j=1}^{(N+1)C} e^{\alpha(x_i, j)} - e^{\alpha(x_i, y_i)} \sum_{j=1}^{(N+1)C} W_j e^{\alpha(x_i, j)}}{e^{\alpha(x_i, y_i)} (\sum_{j=1}^{(N+1)C} e^{\alpha(x_i, j)})^2} \\ &= W_{y_i} - \frac{\sum_{j=1}^{(N+1)C} e^{\alpha(x_i, j)} W_j}{\sum_{j=1}^{(N+1)C} e^{\alpha(x_i, j)}} \end{aligned} \quad (\text{xv})$$

During training process, the class weights of past and present tend to be close each other, leading to the conclusion of $e^{\alpha(x_i, y_i)} \gg e^{\alpha(x_i, j)}$ for $j \neq y_i^{(n)}$, where $y_i^{(n)}$ with $n = 1, 2, 3, \dots, N$ represents the virtual classes of class y_i from the step n and the term $y_i^{(0)} = y_i$ is used for convenience. By applying such conclusion to the numerator of Equation xv for approximation, following equation can be achieved:

$$\begin{aligned} \frac{\partial l_{MemVir}(x_i, y_i)}{\partial x_i} &= W_{y_i} - \frac{\sum_{j=1}^{(N+1)C} e^{\alpha(x_i, j)} W_j}{\sum_{j=1}^{(N+1)C} e^{\alpha(x_i, j)}} \\ &\approx W_{y_i} - \frac{\sum_{n=0}^N e^{\alpha(x_i, y_i^{(n)})} W_{y_i^{(n)}}}{\sum_{j=1}^{(N+1)C} e^{\alpha(x_i, j)}} \\ &= \tau_0 W_{y_i} + \sum_{n=1}^N \tau_n W_{y_i^{(n)}}, \end{aligned} \quad (\text{xvi})$$

$$\tau_0 = 1 - \frac{e^{\alpha(x_i, y_i)}}{\sum_{j=1}^{(N+1)C} e^{\alpha(x_i, j)}}, \tau_n = -\frac{e^{\alpha(x_i, y_i^{(n)})}}{\sum_{j=1}^{(N+1)C} e^{\alpha(x_i, j)}} \quad (\text{xvii})$$

It is obvious that $\tau_0 > 0$. However, τ_0 would not be close to zero whether x_i is nearby W_{y_i} or not, because virtual classes would be close to W_{y_i} . This can alleviate the phenomenon of the embedding feature becoming extremely close to the target W_{y_i} . In addition, because of τ_n , such alleviation would be more extensive and can effectively ease the intense focus of the softmax loss, leading to a more substantial generalization.

B.2. Revisiting Slow Drift Phenomena

“Slow drift” phenomena have been introduced in [32], which identifies the slow drifting speed of the embeddings by measuring the difference of features for the same instance computed at different training steps. With this observation, [32] suggests using the embeddings of past steps for loss computation of the current step. We reproduce “slow drift” phenomena with weight features as follows:

$$\triangle d(W_t, W_{t-m}) := \|W_t - W_{t-(m+1)}\|_2^2, \quad (\text{xviii})$$

where W_t is weight features of current step t and $W_{t-(m+1)}$ is weight features of past step $t - (m + 1)$. As illustrated in Figure A, the weight drift of the baseline is very slow, especially after learning rate decay. We can observe that it converges to local minima with a negligible amount of weight updates after the learning rate decay. On the contrary, when we turn on MemVir instead of learning rate decay, we observe that the weight drift has risen by the enlarged magnitude of gradient; thus, it gives more chance to escape from the local minima for performance improvement.

We further analyze these phenomena by comparing the gradient descent of the softmax loss and MemVir. The softmax

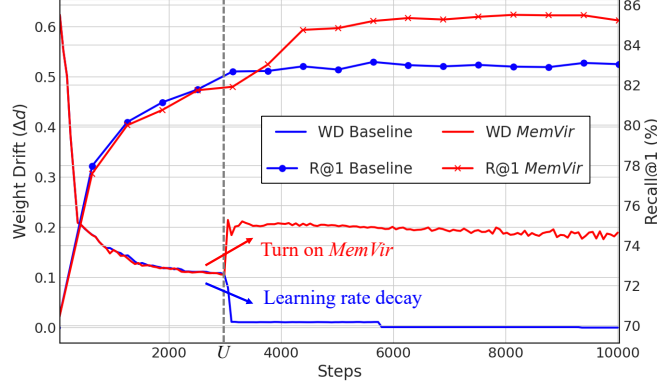


Figure A. Weight drift Δd with $m = 100$ and corresponding Recall@1 performance of baseline and MemVir(1,100).

loss can be written as follows:

$$\begin{aligned}
 l_{softmax}(x_i, y_i) &= \log \frac{e^{W_{y_i}^T x_i}}{\sum_{j=1}^C e^{W_j^T x_i}} \\
 &= \log \frac{e^{\alpha(y_i, i)}}{\sum_{j=1}^C e^{\alpha(j, i)}}, \tag{xix}
 \end{aligned}$$

where $\alpha(j, i) = W_j^T x_i$. Then, the gradient of such loss over $\alpha(j, i)$ can be inducted as follows:

$$\begin{aligned}
 \frac{\partial l_{softmax}(x_i, y_i)}{\partial \alpha(y_i, i)} &= \frac{\sum_{j=1}^C e^{\alpha(j, i)} - e^{\alpha(y_i, i)}}{\sum_{j=1}^C e^{\alpha(j, i)}} \\
 &= 1 - \frac{e^{\alpha(y_i, i)}}{\sum_{j=1}^C e^{\alpha(j, i)}}. \tag{xx}
 \end{aligned}$$

Because $e^{\alpha(y_i, i)} \gg e^{\alpha(j, i)}$ for $j \neq y_i$, thus, $\frac{\partial l_{softmax}(x_i, y_i)}{\partial \alpha(y_i, i)}$ is close to zero. Considering the weight update is performed by $w = w - \eta \frac{\partial L}{\partial w}$, where η is a learning rate, the weight update will be negligible and result in “slow drift” phenomena, especially with a small learning rate.

MemVir overcomes such situation by increasing the magnitudes of gradients. The inducted gradient of MemVir over $\alpha(j, i)$ is as follows:

$$\begin{aligned}
 \frac{\partial l_{softmax}(x_i, y_i)}{\partial \alpha(y_i, i)} &= \frac{\sum_{j=1}^{(N+1)C} e^{\alpha(j, i)} - e^{\alpha(y_i, i)}}{\sum_{j=1}^{(N+1)C} e^{\alpha(j, i)}} \\
 &= 1 - \frac{e^{\alpha(y_i, i)}}{\sum_{j=1}^{(N+1)C} e^{\alpha(j, i)}} \\
 &\approx 1 - \frac{e^{\alpha(y_i, i)}}{e^{\alpha(y_i, i)} + \sum_{n=1}^N e^{\alpha(y_i^{(n)}, i)}}, \tag{xxi}
 \end{aligned}$$

where $y_i^{(n)}$ is the index of the weights before n steps. As $e^{\alpha(y_i^{(n)}, i)}$ are not close to zero, $\frac{\partial l_{softmax}(x_i, y_i)}{\partial \alpha(y_i, i)}$ will not be close to zero. Thus, the gradient of MemVir will be relatively larger than that of the softmax loss, which gives more chance to escape from the local minima. Note that the magnitudes of gradients can be controlled by the difficulty of curriculum learning, such as hyper-parameters N and M .

	Softmax	ArcFace	CurricularFace
CARS196	(30, 50)	(40,50)	(5,100)
SOP	(4, 50)	(10,50)	(9,50)

(a) Comparison with related methods.

	Softmax	Norm-softmax	CosFace	ArcFace	Proxy-NCA	Proxy-anchor
CUB200	(5,75)	(10,10)	(25,150)	(40,40)	(10,25)	(5,75)
CARS196	(15,25)	(45,10)	(25,150)	(15,10)	(20,25)	(15,75)
SOP	(3,150)	(7,90)	(6,100)	(9,80)	(2,80)	(8,50)

(b) Conventional evaluation.

	Norm-softmax	CosFace	ArcFace	Proxy-NCA	Proxy-anchor
CUB200	(15,20)	(35,75)	(40,100)	(40,50)	(15,75)
CARS196	(50,50)	(2,300)	(35,10)	(10,250)	(25,25)
SOP	(15,50)	(10,50)	(5,200)	(20,50)	(5,100)

(c) MLRC evaluation.

Table A. Hyper-parameters (N, M) of MemVir for each experiment.

C. Details of Experimental Settings

C.1. Datasets

Throughout the paper, we use three famous benchmarking datasets in deep metric learning (DML) as follows:

- CUB200-2011 (CUB200) [27]: CUB200 contains 11,788 images of birds in 200 classes. We use 5,864 images of the first 100 classes for training and 5,924 images of the other 100 classes for testing without bounding box information.
- CARS196 [16]: CARS196 contains 16,185 images of cars in 196 classes. We use 8,054 images of the first 98 classes for training and 8,131 images of the other 98 classes for testing without bounding box information.
- Stanford Online Products (SOP) [21]: SOP contains 120,053 images of products in 22,634 classes. We use 59,551 images of the 11,318 classes for training and 60,502 images of the other 11,316 classes for testing.

C.2. Implementation

We implement all models using the PyTorch framework [23], and experiments are performed on Nvidia V100 GPUs. For the *conventional evaluation*, we follow the widely used training and testing protocol as [21, 25, 11, 30]. For the *Metric Learning Reality Check (MLRC) evaluation*, we follow the training and evaluation procedure defined in [20].

C.2.1 Conventional Evaluation

Input images are augmented by random cropping and horizontal flipping in the training phase, whereas they are center-cropped in the test phase. The size of the cropped images is 224×224 . For the backbone network, the Inception network with batch normalization (BN-Inception) [9] pre-trained with ImageNet [1] is used. We use a global average pooling followed by a fully connected layer for dimensionality reduction and set the dimension of the embedding feature to 512. We freeze batch normalization for CUB200 and CARS196 and keep batch normalization training for SOP by following [24, 30, 11]. The batch size is set to 128 for every experiment. Optimization is performed using Adam optimizer [14] with a learning rate of 10^{-4} for CUB200 and CARS196, and 10^{-3} for SOP. The learning rate is decayed by a factor of 0.1 at the 50th epoch for CARS196, and the 20th epoch for CUB200 and SOP. For MemVir, we use warm-up epoch $U_e = 50$ for CARS196 and SOP, and $U_e = 20$ for CUB200 without learning rate decay. With the same hyper-parameters of the baselines, we tune hyper-parameters N and M for MemVir via hyper-parameter search as described in A.

Proxy-anchor: For more details of Proxy-anchor loss in terms of implementation, we have found that proxy-anchor loss has been implemented with additional tricks, which is also mentioned in [35]. The additional tricks are as follows: 1) an AdamW optimizer [17] instead of Adam optimizer [14], 2) a parameter warm-up strategy for better optimization stability, 3) instead of an average pooling, a combination of an average and a max pooling following the backbone network. For a fair comparison, we discard those tricks and follow the conventional metric learning protocol in every experiment. Exceptionally, we use the parameter warm-up with one epoch for SOP dataset because the training with Proxy-anchor loss fails without the parameter warm-up strategy.

Multi-Similarity loss: In Multi-Similarity (MS) loss [30], we have found that the best scores reported in the paper are conducted with either too small or large batch size, such as a batch size of 80 for CUB200 and batch size of 1000 for SOP. For a fair comparison, we conduct experiments of MS loss with the conventional batch size of 128., including the number of instances of 4. Note that we use the number of instances of 4 instead of 5 from the paper because 128 is not divisible by 5.

C.2.2 MLRC Evaluation

Each image is resized to make its shorter side to be the length of 256, then augmented by random cropping to have a size between 40 and 256, and by aspect ratio between 3/4 and 4/3 in the training phase. The resulting image is then resized to 227×227 and flipped horizontally with a 50% probability. In the test phase, each image is resized to 256 and center-cropped to 227. We use BN-Inception for the backbone network with an output embedding size of 128. Optimization is performed using RMSprop optimizer with a learning rate of 10^{-6} and a batch size of 32. To find the best hyper-parameters for loss functions, we run 50 experiments of hyper-parameter search with 4-fold cross-validation of each experiment. With the best hyper-parameters found, we conduct 10 training runs and report the average and confidence intervals to be less subject to random seed noise. We report both separated (128-dim) and concatenated (512-dim) performance, where the 512-dim embedding is concatenated and l_2 -normalized of 128-dim embedding of the 4 models.

C.3. fANOVA

We apply the fANOVA [8] analysis framework to estimate the impact of each hyper-parameter on the performance of MemVir in Section 4.4 and D.5. fANOVA predicts the marginal performance using a predictive model (random forest), which is a function of the model’s hyper-parameters. Then, it determines the extent to which each hyper-parameter or pair-wise interaction contributes to the model performance. In the experiments of MemVir, we conduct 5 training runs for each pair of (N, M) , and each pair is created by the combination of range N and range M . For CUB200 and CAS196, range N is 5 to 50 in 5 intervals including 1, and range M is 0 to 100 in 10 intervals. For SOP, we reduce the range N to be 1 to 7 because of memory limitation of one gpu. These experimental results are used to train random forests for fANOVA analysis.

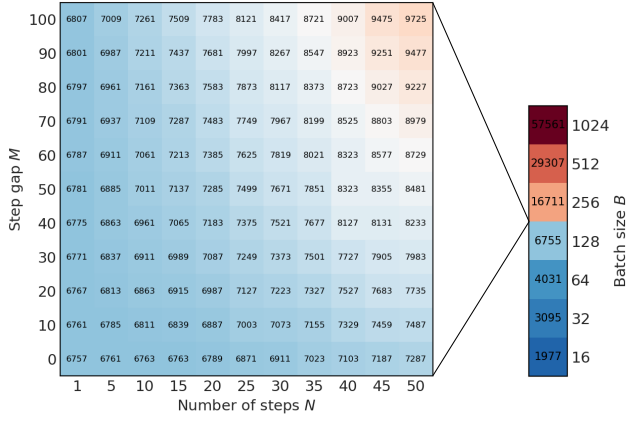
D. Extended Experiments

D.1. Analysis of Memory and Computational Cost

In this section, we analyze memory and computational cost of MemVir with the same experimental setting described in Section C.2.1. MemVir requires $O(BNM(D + C))$ for the memory queues, $O(BCN^2)$ for the similarity matrix, and $O(BCN^2)$ for the computational complexity during the training phase, where B , C , and D are batch size, number of classes, and feature dimension, respectively. In the inference phase, MemVir requires no additional memory or computational cost. As shown in Figure B, the memory usage of MemVir with 128 batch size increases as N and M are increased. Compared to the Norm-softmax model, MemVir(1,100) and MemVir(45,10) improve +1.3% and +3.5% performances with additional 52MB and 704MB GPU memory, respectively. MemVir(50,100), which increases the number of classes and embeddings by 50 times, only requires additional 2.9GB GPU memory and shows better memory efficiency than the baseline with 256 batch size, which requires 6.8GB more GPU memory than MemVir(50,100) with 128 batch size. Even though the memory usage of MemVir would be larger for datasets with a large number of classes, it can be controlled by placing a reduced number of class weights in \mathbb{W} , which are corresponding classes of current step embeddings. In terms of performance, applying MemVir is more effective than increasing the batch size, which is empirically shown in Section 4.3.

D.2. Impact of Learning Rate

Typically, memory-based methods [13, 32] get influenced by learning rate because it affects the difference between training steps. As discussed in Section 3.2, MemVir can control the difference between training steps with margin parameter M . To



(a) $\text{MemVir}(N,M) + \text{Norm-softmax}$ with 128 batch size (b) Norm-softmax

Figure B. Memory usage (MB) of $\text{MemVir}(N,M) + \text{Norm-softmax}$ with 128 batch size and Norm-softmax with different batch size on CARS196 dataset.

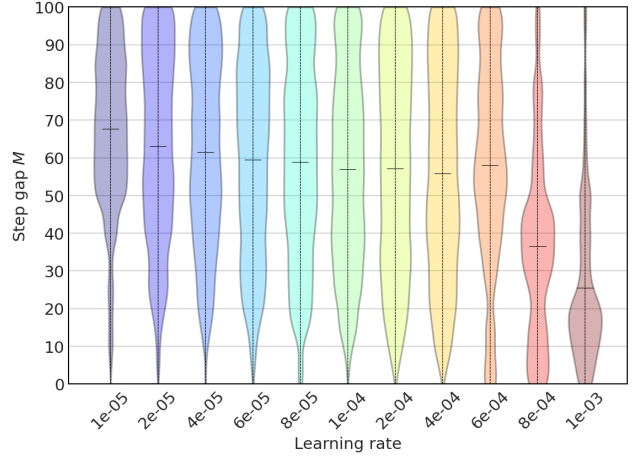


Figure C. Distributions of relative performances for each learning rate by step gap M . For each learning rate, Recall@1 performances of $\text{MemVir}(1,M)$ on CARS196 dataset are normalized across step gap M .

see the impact of learning rate, we train $\text{MemVir}(1,M)$ with a range M from 0 to 100 in 5 intervals and normalize Recall@1 performances across step gap M for each learning rate. We plot the distributions of relative performances by step gap M for each learning rate. As described in Figure C, the larger learning rate requires the smaller step gap M for better performance. This is because a sufficient difference between the training steps can be achieved by a large gap M for a small learning rate and a small gap M for a large learning rate. Thus, the different learning rates can be controlled by the step gap M for MemVir.

D.3. Impact of Warm-up

As discussed in Section 3.3.1, the warm-up period of MemVir enables the model to avoid training with distractive virtual classes from the initial step. To see the impact of the warm-up period, we conduct experiments by differentiating the warm-up epoch with $\text{MemVir}(1,100)$ and $\text{MemVir}(50,10)$. As shown in Figure D, $\text{MemVir}(1,100)$ shows the lowest performance when $U_e = 0$ and stable performance for $U_e > 0$. For $\text{MemVir}(50,10)$, the lowest performance is also shown when $U_e = 0$ and the performance increases until $U_e = 60$, then decreases. It is noteworthy that the lowest performance of MemVir with $U_e = 0$ still shows higher performance than that of the baseline. The results show that proper steps of warm-up help increase the capability of MemVir, and this pattern stands out more to MemVir with longer scheduling of virtual classes addition.

D.4. Robustness to Input Deformation

We now evaluate the quality of representations learned with MemVir with respect to generalization to input deformations. We train models with Norm-softmax loss and MemVir + Norm-softmax loss on CARS196 dataset but test them on the novel (not seen during training) input deformations of the test set. For the input deformation, we use the *imgaug* [10] python library and the details of deformations are as follows.

- *Cutout*: Each image is randomly filled with two gray pixels that are 20% of the image size.
- *Dropout*: $p\%$ of pixels are dropped from each image, where p is randomly sampled from a range $0\% \leq p \leq 20\%$.
- *Zoom-in* and *zoom-out*: Each image is transformed by zoom-in and zoom-out with scale of 50% and 150%, respectively.
- *Rotation* and *shearing*: Each image is transformed by rotation and shearing with a randomly sampled degree between -30° and 30° .
- *Gaussian noise*: Gaussian noise is applied to each image, where the noise is sampled per pixel from a normal distribution $N(0, s)$ and s is sampled between 0 and 0.2×255 .

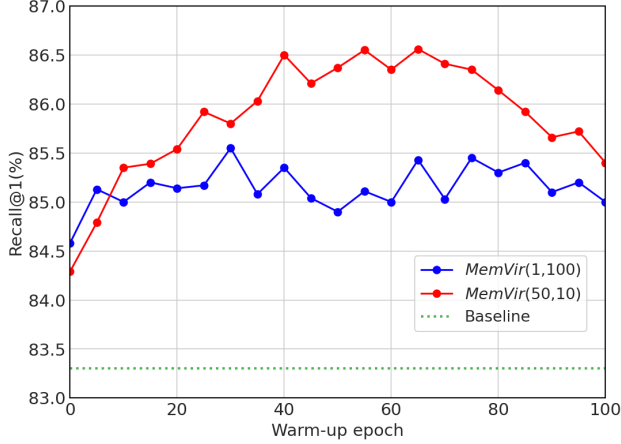


Figure D. Impact of warm-up epoch U_e of MemVir + Norm-softmax on CARS196 dataset. We report the performance of MemVir with different warm-up epoch. Note that the performance of baseline Norm-softmax is unrelated to the warm-up epoch.

Deformation	Norm-softmax	MemVir
W/o deformation	83.3	86.6 (+3.3)
Cutout	75.3	79.2 (+3.9)
Dropout	59.7	67.7 (+8.0)
Zoom in	64.3	68.1 (+3.9)
Zoom out	78.3	81.7 (+3.4)
Rotation	70.8	73.4 (+2.6)
Shearing	70.3	73.2 (+3.0)
Gaussian noise	65.1	71.2 (+6.1)
Gaussian blur	74.4	78.2 (+3.8)

Table B. Recall@1(%) performance of input deformations with CARS196 trained models. We compare Norm-softmax with MemVir(50,10) + Norm-softmax.

(N,M)	(0,0)-baseline	(1,100)	(5,100)	(10,100)	(20,100)
Only-weights		84.4	84.5	84.3	83.8
MemVir	83.6	84.9	85.1	85.5	85.8

Table C. Recall@1 (%) of only-weights and MemVir on CARS196.

- *Gaussian blur*: Gaussian kernel with a sigma of 3.0 is applied to each image.

As shown in Table B, performances of Norm-softmax are degraded significantly when applied input deformations. On the other hand, MemVir exhibits relatively smaller performance degradation compared to that of the Norm-softmax, and shows better robustness to all input deformations, particularly for dropout and gaussian noise. This demonstrates that MemVir allows the model to obtain a more generalized embedding space.

D.5. Impact of Hyper-parameters

In addition to the hyper-parameter analysis of CARS196 in Section 4.4, we include extra analyses on CUB200 and SOP. As shown in Figure E, the performance on CUB200 increases until the margin $M = 5$, and then decreases. For the margin, the performance improves as the margin M increases. In the case of SOP, the performance increases as both N and M increase while there is a slight degradation of performance around $M = 10$. As mentioned in Section 4.4, the performance pattern and importance of each hyper-parameter differs for each dataset because of different data characteristics. However, we can observe that, for both CUB200 and SOP, the best performance is achieved when N and M are larger than 1 and 0, respectively.

D.6. Impact of Embeddings and Class Weights in Virtual Class

To investigate the quantitative impact of embeddings and class weights in virtual classes, we conduct an experiment by using only class weights in virtual classes. Note that using only embeddings in virtual classes is not possible because every embedding requires corresponding class weights in loss computation. Table C shows that using only class weights increases performance than the baseline, but using both embeddings and class weights (MemVir) outperforms it. It suggests the necessity of embeddings to form proper virtual classes.

D.7. Comparison with Related Methods

We provide an extended comparison with related methods from image recognition tasks following Section 4.5. As shown in Table Da, we set two different experimental setups to compare the methods in various experimental settings. Setup 1

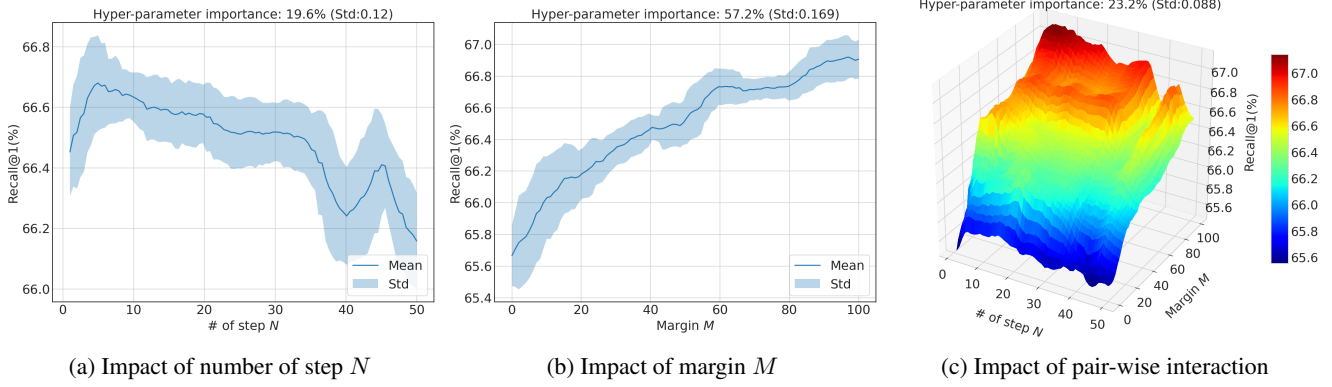


Figure E. Impact of hyper-parameters on CUB200 with fANOVA analysis framework.

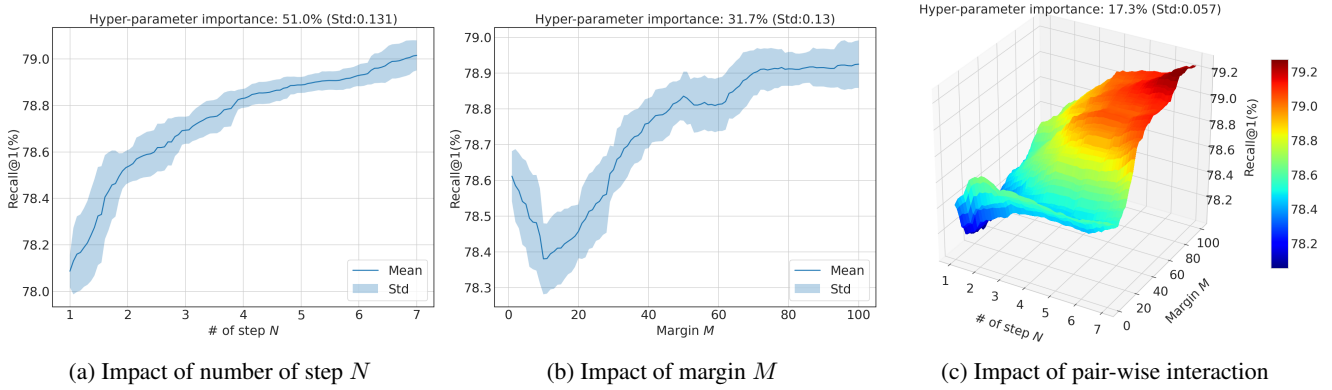


Figure F. Impact of hyper-parameters on SOP with fANOVA analysis framework.

is following the experimental settings from BroadFace [13] and CurricularFace [7], and setup 2 is from the conventional DML settings described in Section C.2.1 with ResNet50 [6] backbone. As XBM [32] shares the memory-based idea with BroadFace, we conduct experiments of XBM in ArcFace loss to compare with BroadFace. As shown in Table D, Virtual softmax degrades the performance for both setups 1 and 2, whereas MemVir improves the performance for both setups. In Virtual softmax, the single virtual class weight is created by $W_{virt} = \frac{\|W_{y_i}\|X_i}{\|X_i\|}$. We observe that the logit with virtual class $W_{virt}^T X_i$ is much larger than the positive logit $W_{y_i}^T X_i$ due to the same direction of vectors W_{virt} and X_i , and it distracts the model from stable training. Combining XBM with ArcFace shows a little performance improvement for both setups, but we observe performance degradation when the memory size is large, as reported in BroadFace. To resolve this problem, BroadFace presents a compensation technique and gradient control. For the details, the compensation technique compensates memorized embeddings by considering class weights updating, while the gradient control computes the loss function into two ways: (1) loss from a mini-batch is for updating the backbone network. (2) loss from the mini-batch and past embeddings is for updating the class weights. BroadFace shows a higher performance boost with the SGD optimizer in setup 1 than the Adam optimizer in setup 2. We observe that BroadFace is sensitive to optimizer type, which could be because of the specifically designed gradient control. On the other hand, MemVir achieves larger performance gains for both setups without any modification of loss functions. CurricularFace shows competitive performance in both setups with an embedded curriculum learning process. When MemVir is applied, the performance of CurricularFace could further be improved by exploiting augmented information from virtual classes.

D.8. Visualization of Embedding Space

For further understanding, we include extended t-SNE [18] visualization of embedding space, followed by Figure 6 in Section 4.2. As illustrated in Figure Ga, Gb, and Gc, embedding features from the seen classes are getting clustered by

	Backbone	Dimension	Batch size	Optimizer	Initial LR
Setup 1	ResNet50	512	512	SGD	0.005
Setup 2	ResNet50	512	128	Adam	0.0001

(a) Two different experimental setups.

Method	CARS196				SOP			
	R@1	R@2	R@4	R@8	R@1	R@10	R@100	R@1000
Softmax	78.3	86.4	91.9	95.7	76.6	89.4	95.8	98.8
Virtual Softmax	75.1	84.1	90.1	94.0	74.5	87.9	94.8	98.3
<i>MemVir</i> + Softmax	79.2	87.0	92.1	95.7	78.9	90.6	96.2	98.8
ArcFace	78.8	86.4	91.7	95.4	76.9	89.1	95.0	98.2
XBM + ArcFace	78.9	86.2	91.9	95.5	78.1	89.7	95.8	98.2
BroadFace + ArcFace	79.5	87.3	92.0	95.5	80.2	91.0	95.9	98.4
<i>MemVir</i> + ArcFace	80.7	88.1	92.7	95.8	80.8	91.3	96.5	98.9
CurricularFace	79.9	87.3	92.0	95.6	79.8	90.7	95.6	98.2
<i>MemVir</i> + CurricularFace	81.0	87.9	92.9	95.8	81.3	91.7	96.5	98.8

(b) Performance (%) comparison in experimental setup 1.

Method	CARS196				SOP			
	R@1	R@2	R@4	R@8	R@1	R@10	R@100	R@1000
Softmax	82.4	88.8	92.1	95.2	78.1	89.1	95.2	97.9
Virtual Softmax	77.6	85.3	90.7	94.3	77.3	87.8	94.1	97.2
<i>MemVir</i> + Softmax	86.8	92.3	95.5	97.6	78.9	90.6	96.2	98.8
ArcFace	83.2	89.5	93.7	96.4	78.6	90.3	95.8	98.5
XBM + ArcFace	83.9	90.3	94.2	96.5	78.8	90.1	96.0	98.3
BroadFace + ArcFace	83.9	90.5	94.2	96.9	79.1	90.7	96.2	98.8
<i>MemVir</i> + ArcFace	85.4	90.9	94.7	96.9	79.5	90.9	96.2	98.8
CurricularFace	83.5	90.1	94.2	96.5	78.5	90.1	95.6	98.4
<i>MemVir</i> + CurricularFace	85.4	91.0	94.5	96.9	79.3	90.5	95.8	98.5

(c) Performance (%) comparison in experimental setup 2.

Table D. Performance (%) comparison with related methods in two different experimental setups.

training process, and further training may cause a model overly fitted to the seen classes. To alleviate this strong focus on seen classes, MemVir begins to add virtual classes slowly and increases learning difficulty gradually, as described in Figure Gd, Ge, Gf, Gg and Gh. Actual and virtual classes, which are originated from the same class label, tend to be located close to each other. Further training allows the model to learn how to discriminate additional classes effectively, as illustrated in Figure Gi, Gj, Gk, and Gl. Finally, we obtain a model with sufficient discriminative power over all actual and virtual classes at the 200th epoch.

D.9. Comparison with State-of-the-art

This section includes extended comparison with state-of-the-art methods for both *conventional evaluation* and *MLRC evaluation* in addition to Section 4.6. As shown in Table E, G, and I of conventional evaluation, we report additional Recall@k performance and comparison with different types of DML methods. For MLRC evaluation, we report both separated (128-dim) and concatenated (512-dim) performance as presented in Table F, H, and J. In conventional evaluation, MemVir shows a significant performance boost in all Recall@k for every dataset and loss function. Compared with different types of DML methods, including ensemble, sample generation, memory-based, pair-based, proxy-based, and softmax variants, MemVir shows competitive performance for all datasets. In MLRC evaluation, MemVir enjoys a high-performance gain over every dataset and loss function in both separated (128-dim) and concatenated (512-dim) experiments. Considering MLRC evaluation is designed for fair evaluation, the results demonstrate that MemVir is a flexible and powerful training strategy for many existing softmax variants and proxy-based losses.

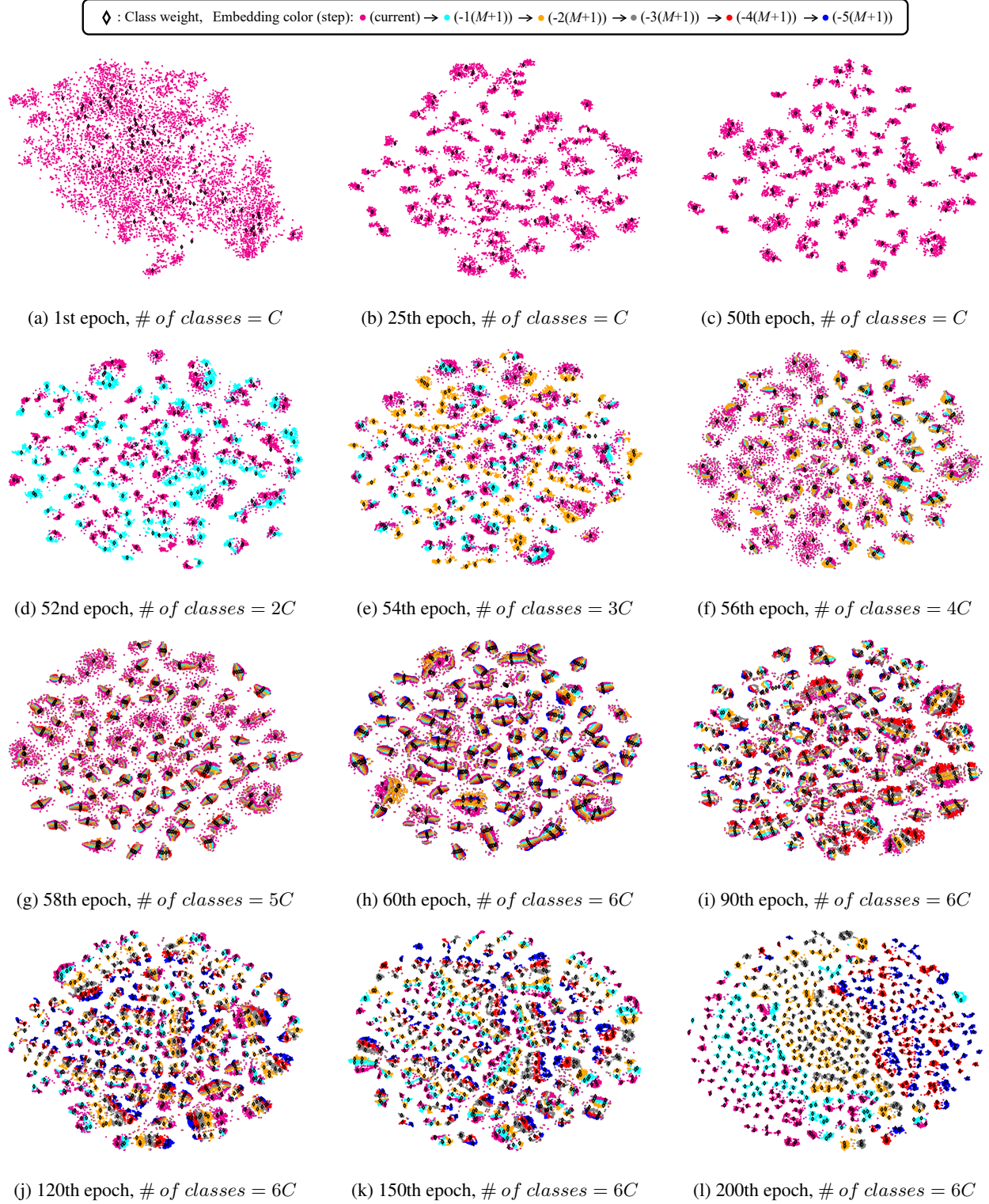


Figure G. t-SNE visualization of 512-dimensional embedding space. Embedding features are extracted by a model trained with MemVir(5,100) on CARS196 training data. Each color indicates a step for embedding features.

CUB-200-2011 [27]											
T	Method	Net	Dim	R@1		R@2		R@4		R@8	
Ens	HDC [33]	G	384	53.6	-	65.7	-	77.0	-	85.6	-
	A-BIER [22]	G	512	57.5	-	68.7	-	78.3	-	86.2	-
	ABE [12]	G	512	60.6	-	71.5	-	79.8	-	87.4	-
Gen	DAML [3] + N-pair	G	512	52.7	-	65.4	-	75.5	-	84.3	-
	HDML [34] + N-pair	G	512	53.7	-	65.7	-	76.7	-	85.7	-
	Symm [5] + N-pair	G	512	55.9	-	67.6	-	78.3	-	86.2	-
	EE [15] + MS	G	512	57.4	-	68.7	-	79.5	-	86.9	-
	Symm [5] + MS	BN	512	64.9	-	76.4	-	84.6	-	90.5	-
	EE [15] + MS	BN	512	65.1	-	76.8	-	86.1	-	91.0	-
M	XBM [32] + Contrastive	BN	512	65.8	-	75.9	-	84.0	-	89.9	-
Pair	HTL [4]	BN	512	57.1	-	68.8	-	78.7	-	86.5	-
	RLL-H [31]	BN	512	57.4	-	69.7	-	79.2	-	86.9	-
	Multi-Similarity (MS) [†] [30]	BN	512	64.5	-	76.2	-	84.6	-	90.5	-
Softmax variant / Proxy	SoftTriple [24]	BN	512	65.4	-	76.4	-	84.5	-	90.4	-
	ProxyGML [35]	BN	512	66.6	-	77.6	-	86.4	-	-	-
	Softmax	BN	512	64.2	-	75.7	-	84.1	-	89.9	-
	MemVir + Softmax	BN	512	66.8	(+2.6)	76.9	(+1.2)	85.4	(+1.3)	91.2	(+1.3)
	Norm-softmax [28]	BN	512	64.9	-	75.7	-	84.3	-	90.5	-
	MemVir + Norm-softmax	BN	512	67.3	(+2.4)	77.2	(+1.5)	85.3	(+1.0)	90.8	(+0.3)
	Cosface [29]	BN	512	65.7	-	76.2	-	84.7	-	90.6	-
	MemVir + Cosface	BN	512	67.7	(+2.0)	77.8	(+1.6)	85.7	(+1.0)	91.1	(+0.5)
	Arcface [2]	BN	512	66.1	-	76.6	-	84.8	-	90.7	-
	MemVir + Arcface	BN	512	67.4	(+1.3)	77.7	(+1.1)	85.5	(+0.7)	91.2	(+0.5)
	Proxy-NCA [19]	BN	512	64.3	-	75.3	-	83.6	-	89.6	-
	MemVir + Proxy-NCA	BN	512	68.3	(+4.0)	78.9	(+3.6)	85.7	(+2.1)	90.9	(+1.3)
	Proxy-anchor [†] [11]	BN	512	67.7	-	78.5	-	85.7	-	90.9	-
	MemVir + Proxy-anchor	BN	512	69.0	(+1.3)	79.2	(+0.7)	86.8	(+1.1)	91.6	(+0.7)
-	Average boost	-	-	-	(+2.3)	-	(+1.6)	-	(+1.2)	-	(+0.8)
	Minimum boost	-	-	-	(+1.3)	-	(+0.7)	-	(+0.7)	-	(+0.3)
	Maximum boost	-	-	-	(+4.0)	-	(+3.6)	-	(+2.1)	-	(+1.3)

Table E. **[Conventional evaluation]** Recall@k (%) on CUB-200-2011 dataset in image retrieval task. Method type (T) is denoted by abbreviations (*Ens*: ensemble, *Gen*: sample generation, *M*: memory-based, *Pair*: pair-based losses, *Softmax variant / Proxy*: softmax variants and proxy-based losses). Backbone network (Net) also is denoted by abbreviations (*G*: GoogleNet [26], *BN*: BN-Inception [9]). [†] denotes evaluation in a fair setting described in Section C.2.1.

CUB-200-2011 [27]		Concatenated (512-dim)			Separated (128-dim)		
Loss		P@1	RP	MAP@R	P@1	RP	MAP@R
Norm-softmax [28]		65.65 ± 0.30	35.99 ± 0.15	25.25 ± 0.13	58.75 ± 0.19	31.75 ± 0.12	20.96 ± 0.11
MemVir + Norm-softmax		69.22 ± 0.15	37.92 ± 0.16	27.10 ± 0.13	59.83 ± 0.23	31.46 ± 0.16	20.55 ± 0.14
CosFace [29]		67.32 ± 0.32	37.49 ± 0.21	26.70 ± 0.23	59.63 ± 0.36	31.99 ± 0.22	21.21 ± 0.22
MemVir + CosFace		69.79 ± 0.26	37.85 ± 0.23	27.08 ± 0.28	61.33 ± 0.30	31.99 ± 0.18	21.30 ± 0.17
ArcFace [2]		67.50 ± 0.25	37.31 ± 0.21	26.45 ± 0.20	60.17 ± 0.32	32.37 ± 0.17	21.49 ± 0.16
MemVir + ArcFace		69.33 ± 0.41	37.82 ± 0.28	26.96 ± 0.25	61.38 ± 0.23	32.53 ± 0.13	21.58 ± 0.12
Proxy-NCA [19]		65.69 ± 0.43	35.14 ± 0.26	24.21 ± 0.27	57.88 ± 0.30	30.16 ± 0.22	19.32 ± 0.21
MemVir + Proxy-NCA		69.25 ± 0.32	37.31 ± 0.12	26.43 ± 0.17	60.08 ± 0.25	31.26 ± 0.15	20.30 ± 0.14
Proxy-anchor [11]		69.73 ± 0.31	38.23 ± 0.37	27.44 ± 0.35	61.50 ± 0.34	32.94 ± 0.25	22.19 ± 0.25
MemVir + Proxy-anchor		69.81 ± 0.28	38.57 ± 0.14	27.83 ± 0.16	62.58 ± 0.28	33.69 ± 0.18	22.75 ± 0.16

Table F. **[MLRC evaluation]** Performance (%) on CUB-200-2011 dataset in image retrieval task. We report the performance of concatenated 512-dim and separated 128-dim. Bold numbers indicate the best score within the same loss.

CARS196 [16]											
T	Method	Net	Dim	R@1		R@2		R@4		R@8	
Ens	HDC [33]	G	384	73.7	-	83.2	-	89.5	-	93.8	-
	A-BIER [22]	G	512	82.0	-	89.0	-	93.2	-	96.1	-
	ABE [12]	G	512	85.2	-	90.5	-	94.0	-	96.1	-
Gen	DAML [3] + N-pair	G	512	75.1	-	83.8	-	89.7	-	93.5	-
	HDML [34] + N-pair	G	512	79.1	-	87.1	-	92.1	-	95.5	-
	Symm [5] + N-pair	G	512	76.5	-	84.3	-	90.4	-	94.1	-
	EE [15] + MS	G	512	76.1	-	84.2	-	89.8	-	93.8	-
	Symm [5] + MS	BN	512	82.4	-	89.2	-	93.3	-	96.1	-
	EE [15] + MS	BN	512	82.7	-	89.2	-	93.8	-	96.4	-
M	XBM [32] + Contrastive	BN	512	82.0	-	88.7	-	93.1	-	96.1	-
Pair	HTL [4]	BN	512	81.4	-	88.0	-	92.7	-	95.7	-
	RLL-H [31]	BN	512	74.0	-	83.6	-	90.1	-	94.1	-
	Multi-Similarity (MS) [†] [30]	BN	512	82.1	-	88.8	-	93.2	-	96.1	-
Softmax variant / Proxy	SoftTriple [24]	BN	512	84.5	-	90.7	-	94.5	-	96.9	-
	ProxyGML [35]	BN	512	85.5	-	91.8	-	95.3	-	-	-
	Softmax	BN	512	81.5	-	89.0	-	93.6	-	96.8	-
	MemVir + Softmax	BN	512	86.5	(+5.0)	92.4	(+3.4)	95.6	(+2.0)	97.4	(+0.6)
	Norm-softmax [28]	BN	512	83.3	-	89.7	-	94.1	-	96.7	-
	MemVir + Norm-softmax	BN	512	86.8	(+3.5)	92.3	(+2.6)	95.4	(+1.3)	97.4	(+0.7)
	Cosface [29]	BN	512	83.6	-	89.9	-	94.2	-	96.6	-
	MemVir + Cosface	BN	512	86.6	(+3.0)	91.8	(+1.9)	95.1	(+0.9)	97.3	(+0.7)
	Arcface [2]	BN	512	83.7	-	90.0	-	94.3	-	96.8	-
	MemVir + Arcface	BN	512	86.5	(+2.8)	91.9	(+1.9)	95.1	(+0.8)	97.1	(+0.3)
	Proxy-NCA [19]	BN	512	82.0	-	89.2	-	93.8	-	96.4	-
	MemVir + Proxy-NCA	BN	512	86.5	(+4.5)	91.8	(+2.6)	95.5	(+1.7)	97.4	(+1.0)
	Proxy-anchor [†] [11]	BN	512	84.9	-	91.1	-	94.6	-	96.9	-
	MemVir + Proxy-anchor	BN	512	86.7	(+1.8)	92.0	(+0.9)	95.2	(+0.6)	97.4	(+0.5)
-	Average boost	-	-	-	(+3.4)	-	(+2.2)	-	(+1.2)	-	(+0.6)
	Minimum boost	-	-	-	(+1.8)	-	(+0.9)	-	(+0.6)	-	(+0.3)
	Maximum boost	-	-	-	(+5.0)	-	(+3.4)	-	(+2.0)	-	(+1.0)

Table G. **[Conventional evaluation]** Recall@k (%) on CARS196 dataset in image retrieval task. Method type (T) is denoted by abbreviations (*Ens*: ensemble, *Gen*: sample generation, *M*: memory-based, *Pair*: pair-based losses, *Softmax variant / Proxy*: softmax variants and proxy-based losses). Backbone network (Net) also is denoted by abbreviations (*G*: GoogleNet [26], *BN*: BN-Inception [9]). [†] denotes evaluation in a fair setting described in Section C.2.1.

CARS196 [16]							
Loss	Concatenated (512-dim)			Separated (128-dim)			
	P@1	RP	MAP@R	P@1	RP	MAP@R	
Norm-softmax [28]	83.16 ± 0.25	36.20 ± 0.26	26.00 ± 0.30	72.55 ± 0.18	29.35 ± 0.20	18.73 ± 0.20	
MemVir + Norm-softmax	85.81 ± 0.18	38.78 ± 0.19	28.92 ± 0.17	76.01 ± 0.23	30.86 ± 0.16	20.36 ± 0.16	
CosFace [29]	85.52 ± 0.24	37.32 ± 0.28	27.57 ± 0.30	74.67 ± 0.20	29.01 ± 0.11	18.80 ± 0.12	
MemVir + CosFace	87.57 ± 0.13	39.10 ± 0.21	29.56 ± 0.26	76.86 ± 0.28	30.59 ± 0.22	20.23 ± 0.24	
ArcFace [2]	85.44 ± 0.28	37.02 ± 0.29	27.22 ± 0.30	72.10 ± 0.37	27.29 ± 0.17	17.11 ± 0.18	
MemVir + ArcFace	88.02 ± 0.18	39.12 ± 0.15	29.63 ± 0.15	78.58 ± 0.26	31.03 ± 0.25	20.89 ± 0.26	
Proxy-NCA [19]	83.56 ± 0.27	35.62 ± 0.28	25.38 ± 0.31	73.46 ± 0.23	28.90 ± 0.22	18.29 ± 0.22	
MemVir + Proxy-NCA	87.02 ± 0.15	38.51 ± 0.15	28.76 ± 0.16	76.35 ± 0.28	30.29 ± 0.23	19.81 ± 0.25	
Proxy-anchor [11]	86.20 ± 0.21	39.08 ± 0.31	29.37 ± 0.29	76.97 ± 0.40	31.71 ± 0.53	21.29 ± 0.56	
MemVir + Proxy-anchor	86.40 ± 0.18	40.27 ± 0.20	30.58 ± 0.20	76.97 ± 0.26	32.87 ± 0.21	22.31 ± 0.22	

Table H. **[MLRC evaluation]** Performance (%) on CARS196 dataset in image retrieval task. We report the performance of concatenated 512-dim and separated 128-dim. Bold numbers indicate the best score within the same loss.

Stanford Online Products [21]											
T	Method	Net	Dim	R@1		R@10		R@100		R@1000	
Ens	HDC [33]	G	384	69.5	-	84.4	-	92.8	-	97.7	-
	A-BIER [22]	G	512	74.2	-	86.9	-	94.0	-	97.8	-
	ABE [12]	G	512	76.3	-	88.4	-	94.8	-	98.2	-
Gen	DAML [3] + N-pair	G	512	68.4	-	83.5	-	92.3	-	-	-
	HDM [34] + N-pair	G	512	68.7	-	83.2	-	92.4	-	-	-
	Symm [5] + N-pair	G	512	73.2	-	86.7	-	94.8	-	-	-
	EE [15] + MS	G	512	78.1	-	90.3	-	95.8	-	-	-
	Symm [5] + MS	BN	512	76.9	-	89.8	-	95.9	-	98.8	-
	EE [15] + MS	BN	512	77.0	-	89.5	-	96.0	-	98.8	-
M	XBM + Contrastive [32]	BN	512	79.5	-	90.8	-	96.1	-	98.7	-
Pair	HTL [4]	BN	512	74.8	-	88.3	-	94.8	-	98.4	-
	RLL-H [31]	BN	512	76.1	-	89.1	-	95.4	-	-	-
	Multi-Similarity (MS) [†] [30]	BN	512	76.3	-	89.7	-	96.0	-	98.8	-
Softmax variant / Proxy	SoftTriple [24]	BN	512	78.3	-	90.4	-	96.0	-	98.3	-
	ProxyGML [35]	BN	512	78.0	-	90.6	-	96.2	-	-	-
	Softmax	BN	512	76.3	-	88.5	-	94.8	-	98.1	-
	MemVir + Softmax	BN	512	77.8	(+1.5)	89.8	(+1.3)	95.4	(+0.6)	98.4	(+0.3)
	Norm-softmax [28]	BN	512	78.6	-	90.5	-	96.0	-	98.6	-
	MemVir + Norm-softmax	BN	512	79.6	(+1.0)	90.9	(+0.4)	96.1	(+0.1)	98.7	(+0.1)
	Cosface [29]	BN	512	78.6	-	90.4	-	95.8	-	98.5	-
	MemVir + Cosface	BN	512	79.7	(+1.1)	90.5	(+0.1)	95.8	(0.0)	98.5	(0.0)
	Arcface [2]	BN	512	78.8	-	90.5	-	95.9	-	98.6	-
	MemVir + Arcface	BN	512	80.0	(+1.2)	90.9	(+0.4)	96.1	(+0.2)	98.7	(+0.1)
	Proxy-NCA [19]	BN	512	78.1	-	90.0	-	95.9	-	98.7	-
	MemVir + Proxy-NCA	BN	512	79.2	(+1.1)	90.4	(+0.4)	96.0	(+0.1)	98.8	(+0.1)
	Proxy-anchor [†] [11]	BN	512	78.9	-	90.6	-	96.1	-	98.5	-
	MemVir + Proxy-anchor	BN	512	79.7	(+0.8)	91.0	(+0.4)	96.3	(+0.2)	98.6	(+0.1)
-	Average boost	-	-	-	(+1.1)	-	(+0.5)	-	(+0.2)	-	(+0.1)
	Minimum boost	-	-	-	(+0.8)	-	(+0.1)	-	(0.0)	-	(0.0)
	Maximum boost	-	-	-	(+1.5)	-	(+1.3)	-	(+0.6)	-	(+0.3)

Table I. **[Conventional evaluation]** Recall@k (%) on Stanford Online Products dataset in image retrieval task. Method type (T) is denoted by abbreviations (*Ens*: ensemble, *Gen*: sample generation, *M*: memory-based, *Pair*: pair-based losses, *Softmax variant / Proxy*: softmax variants and proxy-based losses). Backbone network (Net) also is denoted by abbreviations (*G*: GoogleNet [26], *BN*: BN-Inception [9]). [†] denotes evaluation in a fair setting described in Section C.2.1.

SOP [21]	Concatenated (512-dim)			Separated (128-dim)		
Loss	P@1	RP	MAP@R	P@1	RP	MAP@R
Norm-softmax [28]	75.67 ± 0.17	50.01 ± 0.22	47.13 ± 0.22	71.65 ± 0.14	45.32 ± 0.17	42.35 ± 0.16
MemVir + Norm-softmax	75.77 ± 0.20	50.24 ± 0.22	47.45 ± 0.25	71.97 ± 0.15	45.47 ± 0.14	42.44 ± 0.14
CosFace [29]	75.79 ± 0.14	49.77 ± 0.19	46.92 ± 0.19	70.71 ± 0.19	43.56 ± 0.21	40.69 ± 0.21
MemVir + CosFace	75.88 ± 0.27	49.95 ± 0.37	47.18 ± 0.38	70.25 ± 0.18	43.82 ± 0.20	40.91 ± 0.19
ArcFace [2]	76.20 ± 0.27	50.27 ± 0.38	47.41 ± 0.40	70.88 ± 1.51	44.00 ± 1.26	41.11 ± 1.22
MemVir + ArcFace	76.05 ± 0.30	50.56 ± 0.33	47.75 ± 0.32	71.18 ± 0.27	44.31 ± 0.28	41.26 ± 0.28
Proxy-NCA [19]	75.89 ± 0.17	50.10 ± 0.22	47.22 ± 0.21	71.30 ± 0.20	44.71 ± 0.21	41.74 ± 0.21
MemVir + Proxy-NCA	76.97 ± 0.31	50.81 ± 0.26	48.02 ± 0.27	72.11 ± 0.25	44.82 ± 0.22	41.93 ± 0.18
Proxy-ancho [11]	75.37 ± 0.15	50.19 ± 0.14	47.25 ± 0.15	71.56 ± 0.11	46.13 ± 0.21	43.03 ± 0.21
MemVir + Proxy-anchor	77.80 ± 0.17	53.21 ± 0.12	50.35 ± 0.13	74.30 ± 0.18	48.94 ± 0.16	45.93 ± 0.15

Table J. **[MLRC evaluation]** Performance (%) on Stanford Online Products dataset in image retrieval. We report the performance of concatenated 512-dim and separated 128-dim. Bold numbers indicate the best score within the same loss.

References

- [1] Jia Deng, Wei Dong, Richard Socher, Li-Jia Li, Kai Li, and Li Fei-Fei. Imagenet: A large-scale hierarchical image database. In *2009 IEEE conference on computer vision and pattern recognition*, pages 248–255. Ieee, 2009. [vi](#)
- [2] Jiankang Deng, Jia Guo, Niannan Xue, and Stefanos Zafeiriou. Arcface: Additive angular margin loss for deep face recognition. In *Proceedings of the IEEE Conference on Computer Vision and Pattern Recognition*, pages 4690–4699, 2019. [ii](#), [xiii](#), [xiv](#), [xv](#)
- [3] Yueqi Duan, Wenzhao Zheng, Xudong Lin, Jiwen Lu, and Jie Zhou. Deep adversarial metric learning. In *Proceedings of the IEEE Conference on Computer Vision and Pattern Recognition*, pages 2780–2789, 2018. [xiii](#), [xiv](#), [xv](#)
- [4] Weifeng Ge. Deep metric learning with hierarchical triplet loss. In *Proceedings of the European Conference on Computer Vision (ECCV)*, pages 269–285, 2018. [xiii](#), [xiv](#), [xv](#)
- [5] Geonmo Gu and Byungsoo Ko. Symmetrical synthesis for deep metric learning. *arXiv preprint arXiv:2001.11658*, 2020. [xiii](#), [xiv](#), [xv](#)
- [6] Kaiming He, Xiangyu Zhang, Shaoqing Ren, and Jian Sun. Deep residual learning for image recognition. In *Proceedings of the IEEE conference on computer vision and pattern recognition*, pages 770–778, 2016. [x](#)
- [7] Yuge Huang, Yuhan Wang, Ying Tai, Xiaoming Liu, Pengcheng Shen, Shaoxin Li, Jilin Li, and Feiyue Huang. Curricularface: adaptive curriculum learning loss for deep face recognition. In *Proceedings of the IEEE/CVF Conference on Computer Vision and Pattern Recognition*, pages 5901–5910, 2020. [iii](#), [x](#)
- [8] Frank Hutter, Holger Hoos, and Kevin Leyton-Brown. An efficient approach for assessing hyperparameter importance. In *International conference on machine learning*, pages 754–762. PMLR, 2014. [vii](#)
- [9] Sergey Ioffe and Christian Szegedy. Batch normalization: Accelerating deep network training by reducing internal covariate shift. *arXiv preprint arXiv:1502.03167*, 2015. [vi](#), [xiii](#), [xiv](#), [xv](#)
- [10] Alexander B. Jung, Kentaro Wada, Jon Crall, Satoshi Tanaka, Jake Graving, Christoph Reinders, Sarthak Yadav, Joy Banerjee, Gábor Vecsei, Adam Kraft, Zheng Rui, Jirka Borovec, Christian Vallentin, Semen Zhydenko, Kilian Pfeiffer, Ben Cook, Ismael Fernández, François-Michel De Rainville, Chi-Hung Weng, Abner Ayala-Acevedo, Raphael Meudec, Matias Laporte, et al. imgaug. <https://github.com/aleju/imgaug>, 2020. Online; accessed 01-Feb-2020. [viii](#)
- [11] Sungyeon Kim, Dongwon Kim, Minsu Cho, and Suha Kwak. Proxy anchor loss for deep metric learning. *arXiv preprint arXiv:2003.13911*, 2020. [ii](#), [vi](#), [xiii](#), [xiv](#), [xv](#)
- [12] Wonsik Kim, Bhavya Goyal, Kunal Chawla, Jungmin Lee, and Keunjoo Kwon. Attention-based ensemble for deep metric learning. In *Proceedings of the European Conference on Computer Vision (ECCV)*, pages 736–751, 2018. [xiii](#), [xiv](#), [xv](#)
- [13] Yonghyun Kim, Wonpyo Park, and Jongju Shin. Broadface: Looking at tens of thousands of people at once for face recognition. *arXiv preprint arXiv:2008.06674*, 2020. [vii](#), [x](#)
- [14] Diederik P Kingma and Jimmy Ba. Adam: A method for stochastic optimization. *arXiv preprint arXiv:1412.6980*, 2014. [vi](#), [vii](#)
- [15] Byungsoo Ko and Geonmo Gu. Embedding expansion: Augmentation in embedding space for deep metric learning. In *Proceedings of the IEEE/CVF Conference on Computer Vision and Pattern Recognition*, pages 7255–7264, 2020. [xiii](#), [xiv](#), [xv](#)
- [16] Jonathan Krause, Michael Stark, Jia Deng, and Li Fei-Fei. 3d object representations for fine-grained categorization. In *Proceedings of the IEEE international conference on computer vision workshops*, pages 554–561, 2013. [vi](#), [xiv](#)
- [17] Ilya Loshchilov and Frank Hutter. Decoupled weight decay regularization. *arXiv preprint arXiv:1711.05101*, 2017. [vii](#)
- [18] Laurens van der Maaten and Geoffrey Hinton. Visualizing data using t-sne. *Journal of machine learning research*, 9(Nov):2579–2605, 2008. [x](#)
- [19] Yair Movshovitz-Attias, Alexander Toshev, Thomas K Leung, Sergey Ioffe, and Saurabh Singh. No fuss distance metric learning using proxies. In *Proceedings of the IEEE International Conference on Computer Vision*, pages 360–368, 2017. [ii](#), [xiii](#), [xiv](#), [xv](#)
- [20] Kevin Musgrave, Serge Belongie, and Ser-Nam Lim. A metric learning reality check. *arXiv preprint arXiv:2003.08505*, 2020. [vi](#)
- [21] Hyun Oh Song, Yu Xiang, Stefanie Jegelka, and Silvio Savarese. Deep metric learning via lifted structured feature embedding. In *Proceedings of the IEEE conference on computer vision and pattern recognition*, pages 4004–4012, 2016. [vi](#), [xv](#)
- [22] Michael Opitz, Georg Waltner, Horst Possegger, and Horst Bischof. Deep metric learning with bier: Boosting independent embeddings robustly. *IEEE transactions on pattern analysis and machine intelligence*, 2018. [xiii](#), [xiv](#), [xv](#)
- [23] Adam Paszke, Sam Gross, Francisco Massa, Adam Lerer, James Bradbury, Gregory Chanan, Trevor Killeen, Zeming Lin, Natalia Gimelshein, Luca Antiga, Alban Desmaison, Andreas Kopf, Edward Yang, Zachary DeVito, Martin Raison, Alykhan Tejani, Sasank Chilamkurthy, Benoit Steiner, Lu Fang, Junjie Bai, and Soumith Chintala. Pytorch: An imperative style, high-performance deep learning library. In H. Wallach, H. Larochelle, A. Beygelzimer, F. d’Alché-Buc, E. Fox, and R. Garnett, editors, *Advances in Neural Information Processing Systems 32*, pages 8024–8035. Curran Associates, Inc., 2019. [vi](#)
- [24] Qi Qian, Lei Shang, Baigui Sun, Juhua Hu, Hao Li, and Rong Jin. Softtriple loss: Deep metric learning without triplet sampling. In *Proceedings of the IEEE International Conference on Computer Vision*, pages 6450–6458, 2019. [vi](#), [xiii](#), [xiv](#), [xv](#)
- [25] Kihyuk Sohn. Improved deep metric learning with multi-class n-pair loss objective. In *Advances in neural information processing systems*, pages 1857–1865, 2016. [vi](#)
- [26] Christian Szegedy, Wei Liu, Yangqing Jia, Pierre Sermanet, Scott Reed, Dragomir Anguelov, Dumitru Erhan, Vincent Vanhoucke, and Andrew Rabinovich. Going deeper with convolutions. In *Proceedings of the IEEE conference on computer vision and pattern recognition*, pages 1–9, 2015. [xiii](#), [xiv](#), [xv](#)

- [27] Catherine Wah, Steve Branson, Peter Welinder, Pietro Perona, and Serge Belongie. The caltech-ucsd birds-200-2011 dataset. 2011. [vi](#), [xiii](#)
- [28] Feng Wang, Xiang Xiang, Jian Cheng, and Alan Loddon Yuille. Normface: L2 hypersphere embedding for face verification. In *Proceedings of the 25th ACM international conference on Multimedia*, pages 1041–1049, 2017. [xiii](#), [xiv](#), [xv](#)
- [29] Hao Wang, Yitong Wang, Zheng Zhou, Xing Ji, Dihong Gong, Jingchao Zhou, Zhifeng Li, and Wei Liu. Cosface: Large margin cosine loss for deep face recognition. In *Proceedings of the IEEE Conference on Computer Vision and Pattern Recognition*, pages 5265–5274, 2018. [ii](#), [xiii](#), [xiv](#), [xv](#)
- [30] Xun Wang, Xintong Han, Weilin Huang, Dengke Dong, and Matthew R Scott. Multi-similarity loss with general pair weighting for deep metric learning. In *Proceedings of the IEEE Conference on Computer Vision and Pattern Recognition*, pages 5022–5030, 2019. [vi](#), [vii](#), [xiii](#), [xiv](#), [xv](#)
- [31] Xinshao Wang, Yang Hua, Elyor Kodirov, Guosheng Hu, Romain Garnier, and Neil M Robertson. Ranked list loss for deep metric learning. In *Proceedings of the IEEE Conference on Computer Vision and Pattern Recognition*, pages 5207–5216, 2019. [xiii](#), [xiv](#), [xv](#)
- [32] Xun Wang, Haozhi Zhang, Weilin Huang, and Matthew R Scott. Cross-batch memory for embedding learning. In *Proceedings of the IEEE/CVF Conference on Computer Vision and Pattern Recognition*, pages 6388–6397, 2020. [iv](#), [vii](#), [x](#), [xiii](#), [xiv](#), [xv](#)
- [33] Yuhui Yuan, Kuiyuan Yang, and Chao Zhang. Hard-aware deeply cascaded embedding. In *Proceedings of the IEEE international conference on computer vision*, pages 814–823, 2017. [xiii](#), [xiv](#), [xv](#)
- [34] Wenzhao Zheng, Zhaodong Chen, Jiwen Lu, and Jie Zhou. Hardness-aware deep metric learning. In *Proceedings of the IEEE Conference on Computer Vision and Pattern Recognition*, pages 72–81, 2019. [xiii](#), [xiv](#), [xv](#)
- [35] Yuehua Zhu, Muli Yang, Cheng Deng, and Wei Liu. Fewer is more: A deep graph metric learning perspective using fewer proxies. *arXiv preprint arXiv:2010.13636*, 2020. [vii](#), [xiii](#), [xiv](#), [xv](#)